UNIVERSITY OF OKLAHOMA

GRADUATE COLLEGE

IDENTIFICATION OF EXTREMELY LOW FREQUENCY ERROR COMPONENTS IN THE GLOBAL POSITIONING SYSTEM (GPS)/WIDE AREA AUGMENTATION SYSTEM (WAAS) POSITION SOLUTION

A DISSERTATION

SUBMITTED TO THE GRADUATE FACULTY

in partial fulfillment of the requirements for the

Degree of

DOCTOR OF PHILOSOPHY

By

GERRY MCCARTOR
Norman, Oklahoma
2009

IDENTIFICATION OF EXTREMELY LOW FREQUENCY ERROR COMPONENTS IN THE GLOBAL POSITIONING SYSTEM (GPS)/WIDE AREA AUGMENTATION SYSTEM (WAAS) POSITION SOLUTION

A DISSERTATION APPROVED FOR THE
DEPARTMENT OF ENGINEERING

BY

_____
Dr. John Fagan, Chair

_____
Dr. James Sluss

_____
Dr. J. David Baldwin

_____
Dr. Monte Tull

_____
Dr. Hillel Kumin

Acknowledgements

Without the continual assistance (and persistence) of Professor John Fagan, this work could not have been accomplished. Professor Fagan repeatedly provided support from assisting with data collection efforts to clearing up administrative problems with the Graduate College.

Other key participants in the production of this dissertation were my wife, who despite having to run a business and family, managed to clear significant periods of time for me to work relatively undisturbed, and my children who did their best to let me work in peace (most of the time).

I must also acknowledge the support and encouragement provided by my managers and co-workers at the FAA. It is a great place to work and provided many of the contacts needed to accomplish this work. Support from the other grad students at the GPS lab was also essential to the study.

Last but not least I appreciate the comments and questions presented by my other committee members, Professors Baldwin, Sluss, Tull, and Kumin, which have helped to augment and focus the work.

Table of Contents

List of Tables

List of Figures

Abstract

The Wide Area Augmentation System (WAAS) was intended to "augment" the basic Global Positioning System (GPS) navigation service to the necessary level to support precision approach operations equivalent to the Instrument Landing System (ILS). For a variety of reasons, this has not been achieved. Full implementation of the system will require improvements to all four principal components: accuracy, integrity, availability, and continuity [7], [9]. Previous work has addressed integrity problems by improved algorithms [12]. Availability and continuity have been and may continue to be improved by increasing the number of Wide-area Reference Stations (WRSs) and expanding and improving the geostationary platforms that broadcast the WAAS corrections. This dissertation, for the first time, addresses the needed improvements to the accuracy component by identifying extremely low frequency error components in the WAAS position solution that are of significant magnitude, representing between 10 and 20 per cent of the total error.

This work, for the first time, examines data collected over a multi-year period by several different types of WAAS receivers installed at diverse geographical locations across the WAAS coverage area. This was done both to eliminate any localized phenomena and to allow examination of the data for geographic or seasonal trends. The dissertation identifies hitherto undetected and ignored common spectral error components in all the data. A graphical representation and two separate spectral decomposition techniques are applied to the data to verify the presence of the error components.

Means of applying corrections for these errors are presented as well as areas of future research and investigation. If the corrections identified by this dissertation can be generally applied, the accuracy component of the WAAS will achieve the level necessary to support ILS quality precision approach operations and support further improvements to the integrity component. The corrections that have been identified in this dissertation can be easily implemented in the master station code managed by Raytheon. This will significantly improve the acceptability and usage of WAAS and lead to a cascade of system improvements that can enhance the capabilities of the Federal Aviation Administration's NextGen (Next Generation Air Transportation System) [32].

Chapter 1

Introduction

This dissertation identifies significant extremely low frequency error components in the Wide Area Augmentation System (WAAS) position solution, representing between 10 and 20 per cent of the total error. It suggests methods for applying these corrections that would allow the accuracy of the WAAS to support ILS quality precision approach operations and also support further improvements to the system integrity. This significant improvement to WAAS could lead to a number of system improvements affecting the Federal Aviation Administration's NextGen (Next Generation Air Transportation System) program.

1.1 GPS/WAAS Position Determination

The Global Positioning System (GPS) is a network of satellites and ground infrastructure that provides navigation services over the entire planet (excepting some limited polar areas). Each satellite broadcasts time-tagged messages that include information allowing the satellite orbital position to be determined. Knowing the source position and time of several satellite broadcasts, a receiver can calculate its location. For reasons that will be discussed in Chapter 2, four satellites are required to be in view to calculate the position and altitude of the receiver. Since the satellite constellation is designed and maintained so that there are normally six to ten satellites in view over most of the planet's surface, it is an extremely rare situation for a receiver not to be able to determine its position.

However, a number of errors dilute the precision of the basic GPS solution. These will be discussed in some detail in the next chapter. It was realized fairly early in the system deployment that most of these errors were slowly varying and relatively constant over large geographic areas. This led to the development of a host of "differential" implementations. Differential systems work by determining the errors in the GPS solution at a known geographic position and applying those corrections to the position solutions calculated by another receiver in the same general area. This process is also discussed in more detail in the next chapter.

The two best known differential correction schemes are the Local Area Augmentation System (LAAS) and the Wide Area Augmentation System (WAAS). These two systems have been developed by the Federal Aviation Administration with assistance from a wide variety of commercial and academic interests.

LAAS provides extremely precise positioning information over a relatively small area, at least the airspace used for approaches to one airport. In some cases, approaches to nearby airports will also be covered. LAAS is referred to as a ground based system which means the entire infrastructure (aside from the GPS satellites) is on the ground. Systemic errors inherent in the LAAS would have only very limited effects on the overall National Airspace System (NAS). There are also additional redundancies and crosschecks built into the ground system that supports the LAAS.

WAAS utilizes geostationary satellite broadcasts to transmit corrections based on reports from ground stations spread across North America. These correction messages are available over large geographical areas. Unlike LAAS, systemic errors in the WAAS could potentially affect hundred's or even thousand's of aircraft (at

some future time when equipage is nearly universal) spread over the entire continent. Likewise, anything that could reduce those systemic errors would have large scale positive effects.

1.2 Outline of Dissertation and Original Contributions

This dissertation will address a detailed study of the spectral composition of errors in the position calculations of representative high-end, commercial navigation WAAS receivers located across the country. The focus of the study was identification of extremely long period components of the noise spectrum that might be repeatable and predictable so that additional processing at either the master control station or in the WAAS receiver could correct for those error components.

In Chapter 1 of this work, the basics of GPS and differential GPS have been covered. This section which provides an outline of the entire work and defines the original contributions of the research is also included.

Chapter 2 is a more technical description of many of the algorithms and calculations discussed in Chapter 1. It explains in more detail how differential corrections are determined and how they are applied in a WAAS application and delves into the remaining WAAS error sources in greater detail.

Chapter 3 describes the collection process used to assemble the data processed for the analysis done in this work. The equipment used at the University and in the WAAS reference stations is identified.

In Chapter 4, the processing and analysis of the data is described in detail and a variety of results presented. A graphical analysis routine is described that visually

displayed the effects of interest. Two distinct spectral decomposition methods were applied, the conventional fast Fourier transform method and the wavelet analysis technique. All methods produced similar results.

Chapter 5 further discusses the results in terms of geographic and seasonal effects on the distributions and what significance this may have in terms of implementing a change to the WAAS to incorporate the improvements. The chapter expresses the analysis findings as conclusions.

Chapter 6 suggests future directions for continued research on the topic and identifies lessons learned during the work. Appendix A describes the sites where the source data was collected.

The original contribution of this work is the identification of at least two significant previously unrecognized error components to the WAAS position solution calculations that appear to be predictable and repeatable across the system's coverage area. The errors appear in data collected from several different WAAS receivers and so do not appear to be artifacts of a unique manufacturer's solution algorithm. The work suggests possible methods for incorporating the corrections into the WAAS solutions.

Chapter 2

Theory of GPS and Differential/Augmented GPS

2.1 Basic Theory

The Global Positioning System is a network of satellites and ground infrastructure that provides navigation services over the entire planet [1], [10], [12], [42]. Messages broadcast by each satellite contain the ephemeris or almanac information for that satellite, a very precisely defined time stamp, and the satellite health status as determined by the satellite. The ephemeris or almanac information allows a receiver on the surface or in the air (or in local space for that matter) to precisely define the satellite orbit and its position in an earth-centered, earth-fixed (ECEF) reference frame.

The GPS satellites are in orbits with periods of 11 hours and 58 minutes. So each satellite's daily coverage will move slowly across the surface of the earth with each successive orbit. It will not pass over the same position at the same time of day for roughly a year. This effect keeps any gaps in the system coverage from remaining in the same area for extended periods.

The time stamp lets the receiver know when the satellite was at a particular position and calculate how far away the satellite was when the message was broadcast, assuming the receiver knows the current time very precisely. The health status message allows the receiver to optimize its selection of satellites by eliminating the unhealthy ones. This "health" generally refers to the stability and drift status of the onboard clock and the currency and validity of the onboard ephemeris.

Assuming the receiver knows the time and ignoring any errors in the system, the messages from three satellites should allow the receiver to perfectly define its distance from three perfectly defined points. Each of those distances defines a sphere around a defined point, the satellite position at the time of broadcast. The solution set for the intersection of those three spheres will normally be two points, one of which will not be reasonable. Figure 2.1 shows this graphically. The three spheres, which are of different radii, represent the sets of points equidistant from the satellite source. The intersection between the top two spheres is the white filled ellipse that would be circle if seen from either of the two satellites centers involved. The two heavy dots represent the intersections of that circle with the third sphere. Since the receiver will normally be below the mathematical plane defined by the three satellites, one solution will be on the far side of the plane, placing the receiver in high orbit. This solution can normally be dismissed.

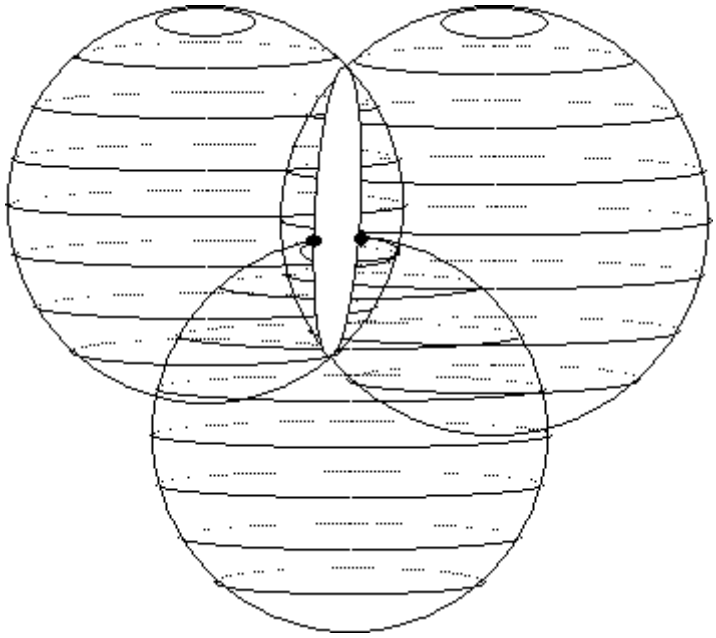

Figure 2.1 Three Satellite Position Solution

However, most receivers are not equipped with atomic clocks like the GPS satellites, so they don't know the time to the necessary precision. (A one micro-second error translates to over eleven hundred feet at the speed of light.) The simplest solution to this problem is to add in another satellite. This makes the math problem more complicated but still solvable and it generally eliminates the unreasonable solution. With four satellites in view, the receiver should be able to precisely define its position. Agreements between the Federal Aviation Administration (FAA), which oversees commercial aviation in the United States, and the Department of Defense, which was responsible for the GPS constellation, dictate that the constellation will have at least 24 active satellites (as of July 2007, there were 30) which should provide five to ten satellites in view over almost all of the planet's surface. It should be very unusual for a receiver with an unobstructed sky view to not be able to calculate its position.

It is not a perfect world. [31] There are considerable variations in ionospheric thickness and tropospheric density which significantly affect the average speed of light between the satellite and the receiver, particularly for low elevation satellites, whose signal passes through more atmosphere. Conversely, if only high elevation satellites are used for a position solution, the quality of the position solution is low due to the geometry. Figure 2.2 graphically represents the atmospheric errors and the relative "depth" of atmosphere for a high elevation satellite versus a low elevation one.

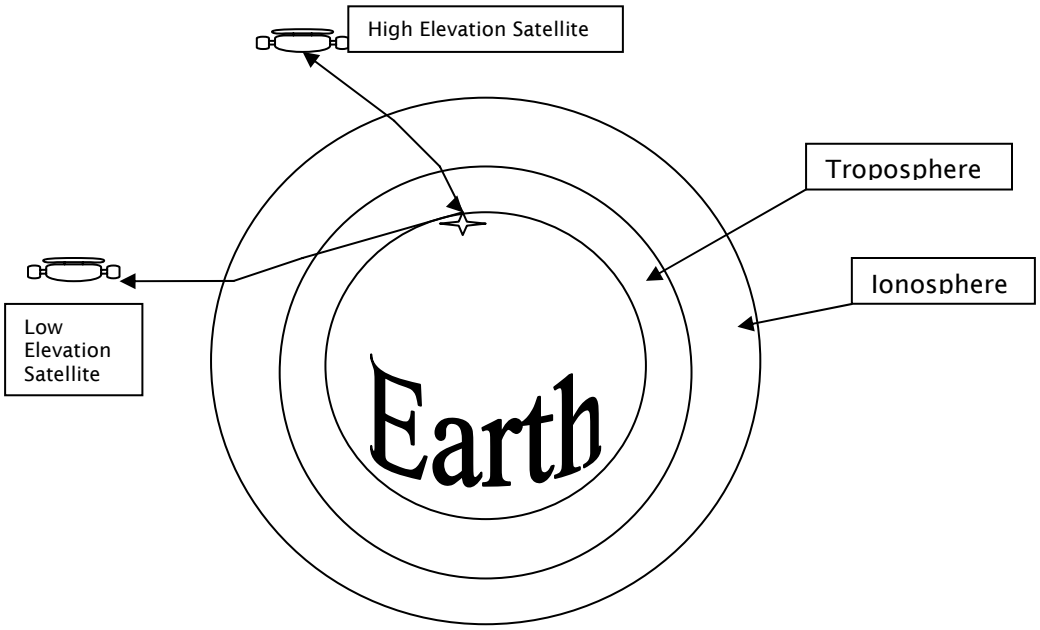

Figure 2.2 Atmospheric Error Sources for GPS Satellites

The gravitational field of the earth is not perfectly uniform resulting in perturbations to the orbital path of the satellites that are not reflected in the ephemeris. The sun and the moon also produce measurable disturbances in the orbits. The atomic clocks on board the satellites do drift and have a certain amount of jitter. Significant changes due to the latter two effects will be detected by the ground infrastructure of the GPS but updates to the clock values or the ephemeris tables are normally only made when the satellites are over the master ground station and only when the errors have reached certain limits. Multipath errors, which occur when signals from the same satellite reach the receiver via different paths (generally after part of the signal was reflected off something), may also contribute significantly. There are also noise and uncompensated delays in the receiver that make a small contribution to the total error. Table 2.1 shows typical values for the various error components [29]. Different sources may quote slight different values.

Table 2.1 Error Sources in GPS Positioning

Source	One σ of range error (m)
Orbit	2.1
Satellite Clock	2.1
Ionosphere	4.0
Troposphere	0.7
Multipath	2.0
Receiver Noise	0.5

When the system was originally deployed, the messages that were accessible to the non-military users contained deliberately corrupted data that reduced the solution accuracy. This was referred to as Selective Availability. Since May of 2000, Selective Availability has been set to zero so that there is no corruption of the base data. [3] (Note that the function has not been turned off or disabled, just turned down to zero.) The combination of these effects reduces the accuracy a pure GPS solution can achieve. Typical solutions are within 15 meters horizontally 95 per cent of the time and 20-25 meters vertically 95 percent of the time (with Selective Availability at 0). Because of the geometric relationship of an earthbound or airborne receiver to the satellite orbits, the vertical position solution is normally about 50 per cent worse than the horizontal. All of the satellites used in a typical position calculation will be "up" from the receiver position, i.e. have a positive elevation, whereas their azimuthal spread can cover a full 360°. This geometric arrangement, referred to as Geometric Dilution of Precision or GDOP, results in (on average) cancellation of more of the lateral error components than the vertical.

If **accuracy** were the only issue, this performance would be pretty phenomenal. No existing navigation system at the time GPS was deployed (or since

then) provided equivalent absolute position information. Various relative positioning systems such as ILS or the Microwave Landing System (MLS) did provide better accuracy for critical applications such as precision approach operations where both horizontal and vertical guidance is required to deliver an aircraft to a point where it can safely land on a runway. But nothing could provide a user with latitude and longitude information of that quality without conducting expensive and time consuming surveying procedures.

Integrity was recognized as an issue very early in the GPS development. [12], [24] If one satellite was broadcasting incorrect information, due to clock or ephemeris errors, it could seriously corrupt the position solution for many receivers. This could be checked by adding more satellites and comparing solutions between different combinations. This process was called Receiver Autonomous Integrity Monitoring (RAIM). Because the parameters for RAIM were established early in the system deployment when the final satellite count was not certain and Selective Availability was still active, fairly coarse levels were selected for the alarms, which were triggered when a receiver reached a state where it could not determine its position to within a certain value. The tightest limit was set to 0.3 nautical miles (nm) or 555 meters, with larger limits of 1 and 5 nautical miles to be used for less critical phases of navigation. The 0.3 nm setting was intended for non-precision approach operations, where no vertical guidance is provided and much coarser lateral guidance is allowed. The higher settings were intended to support operations in the terminal area or en route.

Availability, another system requirement, was largely driven by the satellite count and the constellation geometry. Orbits could be manipulated to maximize

coverage over a particular area for a period of time. This was done in the first Gulf War to support military operations in the Middle East. As the satellite count has continued to increase, availability has not been a problem except in far northern and southern latitudes. The GPS satellite orbits are inclined at 55 degrees with respect to the equator so they never directly pass over the Polar Regions and subsequently availability is limited there.

Continuity can be a problem for certain applications because, when the GPS receiver drops one satellite from its solution matrix and adds another, there is an inevitable jump in the calculated position. This can best be addressed by tailoring the satellite selection algorithms for critical phases of flight so that there won't be any satellite changes or implementing all-in-view solutions that tend to dampen the significance of single satellite changes. The ability to implement these methods is limited by the software complexity and the availability of enough satellites in view.

2.2 Differential GPS

The delay from the satellite broadcast of a time mark to receiver reception is referred to as pseudorange. Errors in GPS position solutions are driven by pseudorange errors. The nature of these pseudorange errors is such that they are relatively constant over a significant geographical area and for significant periods of time. With Selective Availability not a factor, the largest remaining error is due to variations in the ionospheric thickness between the satellite and the receiver. While not understood very well, this is generally a very slowly varying value that does not change rapidly across small distances. Clock drift, another source of error, is

controlled by the satellites internal monitoring. If it starts changing too fast, where "too fast" is still very slow, the satellite will declare itself "unhealthy" and GPS receivers will not use it in the solution. Other effects that produce errors include the tropospheric density and variations in the orbit that are not shown in the ephemeris. None of these errors change very fast or result in effects that are limited to small geographical areas. There are "jitter" components to the pseudorange error but the slowly varying components are the dominant ones. The point of this is that if a correction to a pseudorange could be determined, it would be applicable over a relatively large area and remain accurate for some period of time. The definitions of "relatively large area" and "some period of time" are subject to the requirements for the task at hand.

This concept led to the development of Differential GPS or DGPS. It turns out that determining pseudorange errors is really very simple. If a high quality GPS receiver is installed at a carefully surveyed position, it can determine exactly what the pseudorange for each satellite should be. It has its own position from the survey data (which it will translate to an earth-centered, earth-fixed XYZ coordinate triplet). It has the satellite coordinates based on calculations using data from the received ephemeris. The receiver can calculate what the pseudorange should be and subtract that value from the pseudorange determined from the message received by the satellite. These pseudorange corrections can then be transmitted by some means to suitably equipped DGPS receivers which add the corrections back to the appropriate satellite's measured pseudorange and then calculates a position using the differentially-corrected satellite ranges.

Various schemes were developed to broadcast the differential corrections and other relevant information to the users. The ground station was obviously in a good position to independently evaluate many of the satellite health parameters and could potentially provide improved integrity information. The United States Federal Aviation Administration eventually decided to develop two independent augmentation systems to support precision approach requirements for accuracy and integrity enhancements beyond what was possible with basic GPS. These two systems were the Local Area Augmentation System (LAAS) and the Wide Area Augmentation System (WAAS).

The LAAS is intended to eventually meet the most stringent requirements of low visibility precision approach operations. [18], [21], [23] As mentioned earlier, precision approaches require both horizontal and vertical guidance with the greater accuracy required in the vertical since the aircraft is more likely to encounter an obstacle flying a little low than flying the same distance to the left or right. Precision approaches are generally broken down into categories identified primarily by the minimum decision height they will support. The decision height, or DH, for an approach is the minimum altitude the pilot can descend to without having the runway in sight. For Category I operations ("Cat One"), the minimum allowed DH is 200 feet above the threshold elevation. If the runway elevation is 1300 feet and the pilot executing the approach cannot see the runway when the instruments show the aircraft to be at 1500 feet altitude, he(she) must execute a go-around and either come back and try the landing again or fly to an alternate destination airport that will hopefully have better weather. Cat II operations allow DH's down to 100 feet and Cat III is generally

down to 50 feet but can go all the way to 0 for autoland operations where the airplane is controlled by the autopilot all the way to touchdown. There are additional requirements on both the airport (lighting, runway markings, etc.) and the aircraft (equipment, training, etc.) but the minimum DH is the primary consideration.

LAAS broadcast corrections are intended to be applied only within a limited geographic area to maximize the resultant accuracy. The system includes multiple ground stations for redundancy and cross checking of each other. It broadcasts on a protected navigation frequency that should be safe from interference. The LAAS broadcast includes not only the pseudorange corrections but approach information for all the runways covered by the system, which may include multiple airports, and integrity information on all visible satellites.

2.3 Wide Area Augmentation System

The Wide Area Augmentation System was not designed to achieve the same level of accuracy possible to the LAAS but was intended to support Cat I operations. [1]. [2], [5], [12], [16], [17], [43] The system has recently been approved to do that with some minor adjustments to the usual approach requirements. [9] WAAS messages are sent on the same frequency band as the GPS broadcasts (eliminating the need for a separate antenna and receiver) and are broadcast from several geostationary satellites that provide coverage across almost all of North America. Because the geostationary satellites, referred to as geo's, are in generally equatorial orbits, WAAS coverage in northern Alaska and Canada is not as robust as it is in the continental U.S. In addition to the geo elevation problem, the current network of WAAS reference

ground stations which determine the pseudorange errors does not extend across northern Canada and is comparatively sparse across Alaska.

The WAAS ground infrastructure currently includes 38 ground reference stations located across North America that collect pseudorange, health, and integrity data on all visible satellites and transmit it to the master control station. (Note that the initial system of reference stations that was in place for most of the data included in this study only included 25 stations.) The WAAS master control station uses the pseudorange error data and a model of the ionosphere to calculate ionospheric "depth" over a grid that extends across the WAAS coverage area and also determines an optimal pseudorange correction per satellite. The pseudorange corrections, satellite health information, and ionospheric depth data is sent from the master control station to the geo-stationary satellites from which it is rebroadcast to the user's receivers.

The WAAS enabled receiver determines the optimal satellites to use based on geometry and the health information. (Depending on the particular algorithms used by the receiver, it may well use all visible satellites if they are healthy.) It then applies the pseudorange corrections, calculates additional corrections due to the relevant ionospheric depths (the system maps the effective thickness of the ionosphere using a grid system defined across the coverage area and uses those grid values that are between the receiver position and the relevant satellite), and solves for the antenna's position which can then be translated to the receiver position or the center of mass of the vehicle.

Because each WAAS ground station is providing an independent assessment of the health and accuracy of each satellite being monitored, the overall system integrity

is substantially enhanced. Principally due to this extra monitoring, WAAS is considered an acceptable sole means of navigation by the FAA and instrument operations can be conducted with no other navigation system on board an aircraft. Basic unaugmented GPS requires a backup system such as a VOR (Very High Frequency Omnidirectional Radio) receiver for approved instrument operations.

2.4 Error Sources

Incorporation of the WAAS corrections into the GPS solution substantially reduces or eliminates most of the errors discussed earlier. Typical WAAS position errors are on the order of 2 to 4 meters laterally and 3 to 6 meters vertically, nearly an order of magnitude better than the basic GPS solutions. Clock drift and ephemeris errors are both almost completely compensated for by the pseudorange corrections (although timing errors between the WAAS correction and the GPS pseudoranges creates a new error source, it is very small in comparison). Errors in the ionospheric and tropospheric modeling and multi-path effects on the correction messages or the pseudorange messages become the dominant sources of error.

The WAAS master station estimates the thickness of the ionosphere across the coverage area and beyond by comparing the pseudorange errors from satellites with expected values and inputting the differences into a mathematical model of the ionosphere. If there are, for instance, several satellites with larger than expected pseudoranges in one section of the sky, the model will “thicken” the ionosphere in the grid cells in that section. The model smoothes out any discontinuities based on anomalous pseudorange values in the calculated thicknesses of the grid cells. The

model is subject to errors in the estimated thickness for a given grid cell and errors due to variations across the individual grid cells, which are many miles across. Tropospheric corrections are relatively small, as seen in section 2.1, and generally based only on the satellite elevation which determines the distance the signal travels in the troposphere.

The next generation of GPS satellites (Block IIF) will include dual frequency capabilities that will allow suitably equipped receivers to evaluate the ionospheric and tropospheric errors on their own. However, the first Block IIF satellite has yet to be launched and replacement of the entire constellation will take a number of years.

The GPS and WAAS messages are broadcast from orbit by essentially omni-directional antennas to provide coverage over as wide an area as possible. When the receiver antenna picks up a signal directly from the satellite and also gets a signal that has reflected off some surface not part of the antenna, a condition known as multi-path may exist. This may also happen when something blocks the direct signal and only the reflected signal is received. The receiver may decide that the reflected signal is the correct one, producing a longer pseudorange value for that satellite, thus shifting the position solution by some amount. Multi-path is usually more common from low elevation satellites (which is one reason why most GPS or GPS/WAAS receivers don't use satellites that are within 5 or 10 degrees of the horizon) which means the distance traveled by the reflected signal is not that much greater than the direct signal but it can have a significant effect. The effect of an error in a single pseudorange is also reduced by having more than a minimal set of satellites providing a solution, which is the normal case with the robust constellation in place.

Chapter 3

Data Collection

3.1 University of Oklahoma Data Collection (Initial)

The University of Oklahoma has been involved with the FAA's GPS program since 1994 when the School of Electrical and Computer Engineering teamed up with the School of Aviation to perform flight testing using some of the first available GPS navigation systems [30], [31]. The tests were performed under the sponsorship of the Flight Procedures Development Branch, AFS-420, located in Oklahoma City. AFS-420 is the FAA organization responsible for defining the airspace requirements for all phases of instrument flight operations. The tests provided important information for the development of standards and criteria for airspace requirements for GPS operations. In the late 1990's, those tests were essentially repeated with prototype WAAS receivers replacing the GPS navigation systems on the test aircraft [16], [17], [19].

Since one of the requirements on the WAAS was to support precision approach operations, i.e. provide high quality guidance both laterally and vertically, and the WAAS messages were being broadcast from commercial satellites rather than from government assets (like the GPS satellites), special attention was focused on the WAAS signal in space. Numerous studies were done to examine its continuity, quality, susceptibility to velocity and acceleration effects, etc. [5], [15], [20], [22]. Many of these studies involved the collection of long term data to allow examination of the signals over hours or days or even months. Part of the WAAS program support

at the University was the development of a system to monitor the WAAS solutions from a precisely surveyed ground receiver location and record the errors in those solutions over extended periods of time. One phase of the study generated data collection for an entire year (2001). This archive was one of the key elements in the study undertaken for this research effort.

These early studies were conducted before commercial aviation certified WAAS receivers were available. The University received an STel GSV-1012 from the FAA Technical Center for use during the initial data collection efforts. The unit included two Novatel multi-channel GPS receiver cards, one modified to receive the WAAS differential correction data. The unit then merged the corrections with the pseudoranges from the unmodified Novatel card. It produced one solution per second. This data rate was not considered acceptable for precision approach operations. The minimum data rate believed suitable for supporting precision approach was set at 5 hertz or five independent solutions per second. Later on in the testing program, the University was provided a Rockwell EMAGR (Enhanced Miniaturized Airborne GPS Receiver) that included WAAS capabilities. While the EMAGR did output five solutions per second, four of the five were based on Doppler corrections to the most recent true WAAS solution. True five hertz receivers were not produced for several years. When the EMAGR was available, data was collected at the lab from October 1999 to March 2002. All of the data recorded during this part of the program was at five hertz, i.e. five position solutions per second. However, as noted earlier, four of the five solutions were based on Doppler updates to the actual WAAS position solution calculated by the receiver.

During the time this early WAAS data was collected (1999-2002), the system was still very much in the development stage. The system was being run from the National Satellite Test Bed (NSTB) facilities at the Tech Center, which was a developmental system itself. There were frequent outages and signal irregularities as the system software and hardware was tested and validated. Stanford University was developing an alternate version of the system and on a few occasions, they were allowed to "take over" the control system and use it to broadcast their data.

The data was collected in the GPS lab at the University on systems with limited storage capabilities (by modern standards). The data was generally archived once a day at about the same time of day, potentially introducing artifacts and gaps in the data stream that might affect analysis results. Longer period collections were conducted as larger storage systems became available.

All of these factors made getting a very long term series of valid data points (in excess of 15 to 20 days) very difficult. Fortunately, most of the irregularities were too short term to significantly impact the signal components for which this study was searching.

3.2 FAA Data Collection

The National Satellite Test Bed (NSTB) facility at the FAA William J. Hughes Technical Center near Atlantic City, NJ, served as the center of initial research on WAAS. Before the first WAAS geo's were online, the NSTB served as a pseudo-geo, sending out WAAS messages over a ground based communication network. The NSTB has continued to collect and archive messages and reports from all the WAAS

Reference Stations and the Master Station. The archived data normally includes only the pseudorange errors recorded at each Reference Stations (as well as satellite status and health messages) but for the 12 months following the declaration of operational status in 2003, three dimensional position errors were recorded at all the WAAS ground reference stations. This data was recorded almost continuously. There were breaks due to system problems that generally took out the entire WAAS network for several hours or even days but while it was up, the system provided very accurate and stable data.

The author initially requested four weeks of data from three sites spaced across the WAAS coverage area: Washington, D.C., Kansas City, Missouri, and Seattle, Washington.

After getting generally positive results from the analysis of data from these sites, another request was made for four 30 day periods of data spaced across the first year of operation from seven reference station locations geographically distributed across the WAAS coverage area (of the time). These sites included: Atlanta, Georgia, Boston, Massachusetts, Minneapolis, Minnesota, Houston, Texas, Oklahoma City, Oklahoma, Salt Lake City, Utah, and Los Angeles, California.

3.3 University of Oklahoma Data Collection (Current)

The original data used in this study was collected between 1999 and 2004. In the intervening years, significant upgrades have been made to the GPS/WAAS network. The GPS satellite constellation count has increased by two or three and many older satellites have been replaced with newer versions. The current

geostationary satellites also provide GPS ranging signals, effectively adding another one or two satellites to the mix. The number of ground stations has increased and expanded to both the north and south. These changes have significantly improved the resolution and quality of the ionospheric mapping routines the system uses to provide the iono corrections. There have also been continuous incremental changes in the system software, improving the overall accuracy and integrity of the system.

In light of these enhancements, it was appropriate to examine long term data from the current system and determine if the error components of interest were still present. The University GPS laboratory dedicated an Ashtech GG-12W to recording data from December 2007 thru January 2008 for a four week period. The data were recorded at two hertz and were provided in earth-centered, earth-fixed coordinates rather than latitude, longitude, altitude, like the previous sets. The analysis of this data is discussed in section 4.4.

Chapter 4

Data Analysis

4.1 Visual Analysis

The basis for this study was an observation by the author based on some early long term WAAS error data that there appeared to be a repeated daily pattern to the position solutions. While this observation was dismissed at the time as multi-path, the author was not convinced and began the initial phases of this study. To confirm the existence of an unknown and significant periodic (and therefore, predictable) error component, a visual tool was constructed that plotted error magnitude (represented by grayscale intensity) as a function of time and allowed the user to plot consecutive sequences of data (such as a day's worth of readings) as adjacent rows of pixels in an image.

One of the very first output screens of an early version of this tool is shown as Figure 4.1. The two blocks are plots of a grayscale mapping of the latitude error and the altitude error. The intensity variations are a mapping of -4 meters to +4 meters of position error to 256 grayscales. Error values which are outside the range are shown as colors, either red or green. Each two horizontal row of pixels represents a twenty-four hour period. (Two rows were used to make inter-row differences easier to detect visually.) The blank lines or areas are periods for which no data was available (a serious problem with the early data). The slanted striations represent orbit-based phenomena. The slant is created by the difference between two orbital periods and a 24 hour day, about 4 minutes. The striations are less visible in the altitude plot

because a bias in the data shifted most of the errors into the darker parts of the grayscale.

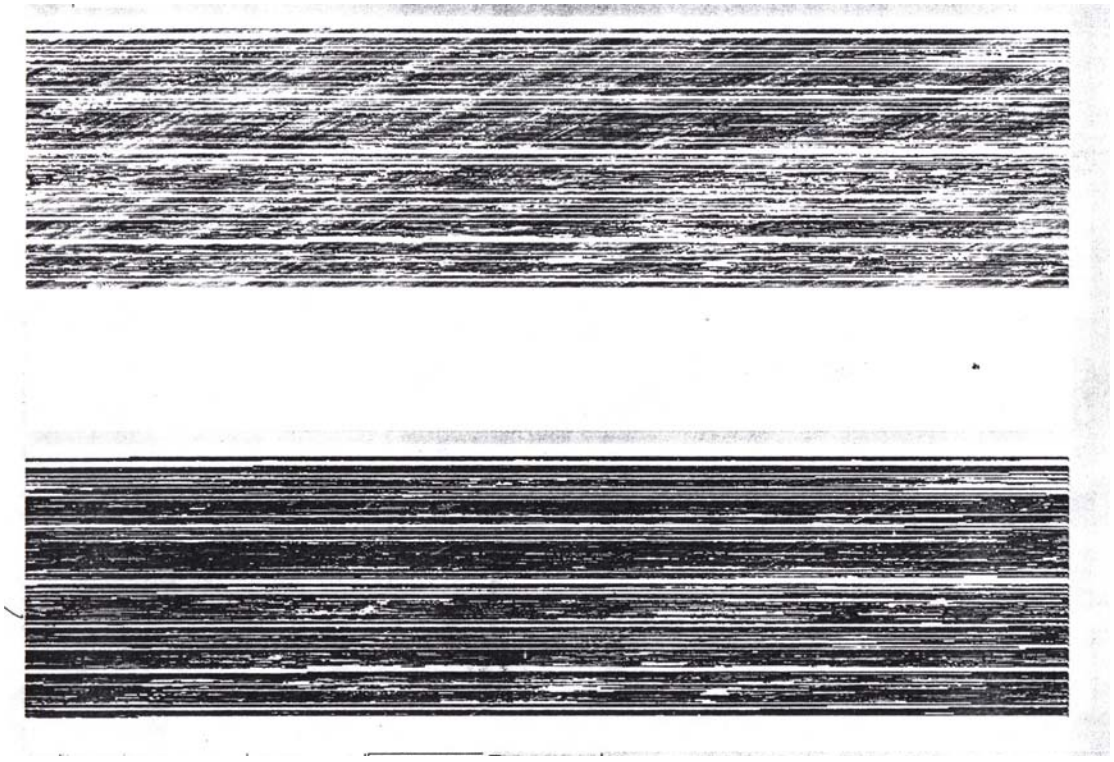

Figure 4.1 Grayscale representation of WAAS latitude and altitude errors for 120 days at Carson Engineering Center (dates unknown but probably late 1999 or early 2000.)

More sophisticated versions of the program allowed the user to simultaneously view data from all three dimensions (latitude, longitude, and altitude) or to look at the same dimension error from three different times or (when the Tech Center data became available from multiple sites) three different locations. By using the tool with different sequence lengths and different time ranges for the input sequences, the author convinced himself (and his advisor) that there were repeated cycles that corresponded to both the solar day and the orbital period (11 hours and 58 minutes). Figures 4.2 through 4.4 show the consistency of certain error components across most of a year at

both Atlanta and Los Angeles in a format similar to Figure 4.1. The error ranges have been adjusted to optimize the grayscale presentation.

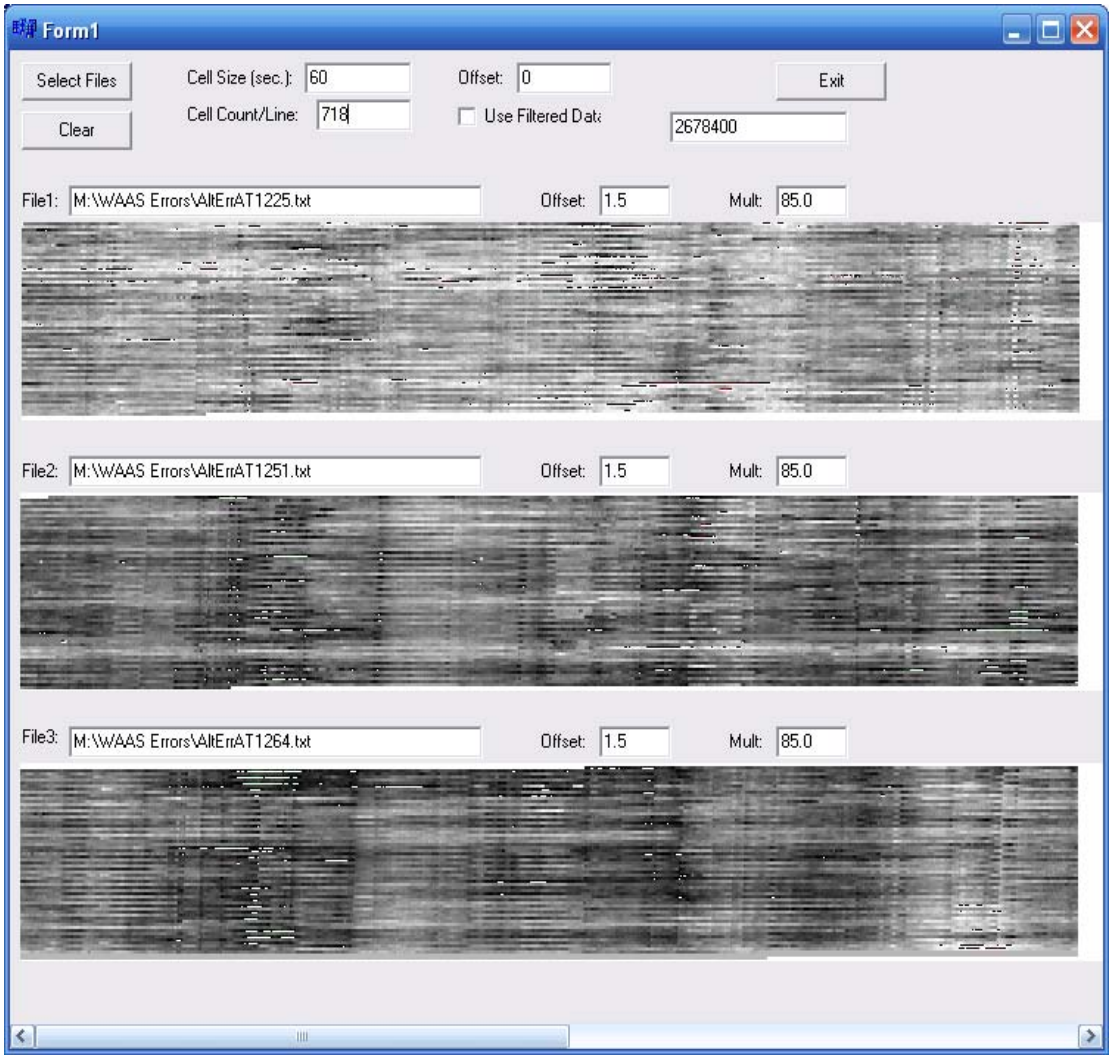

Figure 4.2 WAAS Altitude Errors at Atlanta for 30 Day Periods Starting at Week 1225, Week 1251, and Week 1264 (9 months total). The X-axis represents one orbital period.

While the four figures are dominated by the orbital period features, several artifacts support the existence of a 24 hour effect, most notably the clearly alternating intensities of successive lines, which suggests that each pair of orbits included a period of more positive error followed in the second orbit by a period of more negative errors (or vice versa). These visual depictions make it clear that there is some repeatable

phenomenon occurring that is both significant (based on the scale of the errors involved) and predictable over extended periods of time, if the position solution was two meters off on January 1st at noon, it can be expected to be off in the same direction at noon on February 1st by an amount close to two meters.

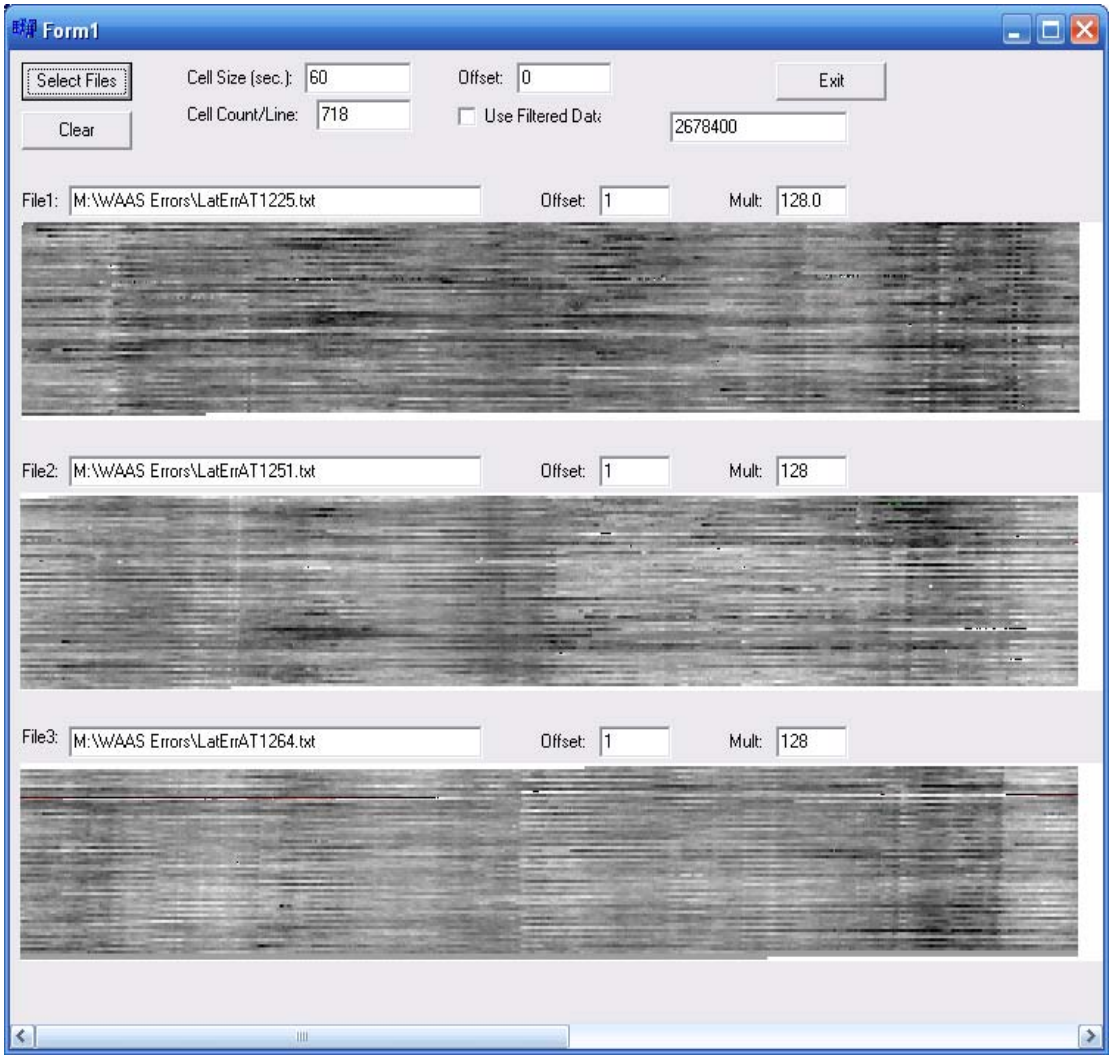

Figure 4.3 WAAS Latitude Errors at Atlanta for 30 Day Periods Starting at Week 1225, Week 1251, and Week 1264 (9 months total). The X-axis represents one orbital period.

Introduction of corrections of this magnitude into the WAAS position solution would be extremely beneficial to the overall system performance. The mathematical

analysis that follows this can determine exact magnitudes and potential phase relationships, but the images shown in these figures really prove the existence of the effect.

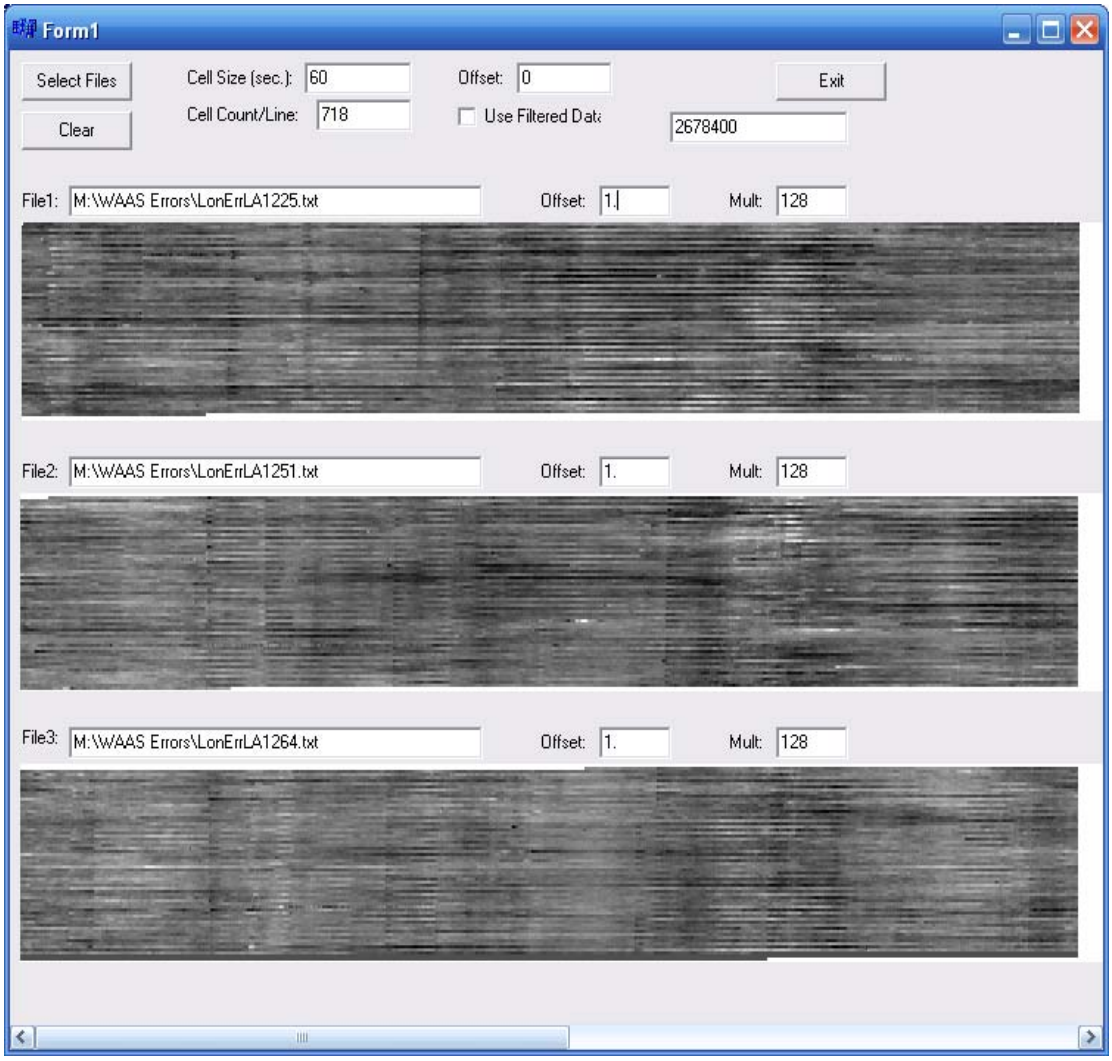

Figure 4.4 WAAS Longitude Errors at Los Angeles for 30 Day Periods Starting at Week 1225, Week 1251, and Week 1264 (9 months total). The X-axis represents one orbital period.

One reasonable explanation of the orbital variations in the error components could be multipath effects. If a particular satellite is in position so that its signal is reflected off of a surface and induces a multipath error at the antenna, it will be in a

similar position on the next orbit. However, many of the variations remain relatively constant over a nine month period, during which there is a substantial shift in the orbital patterns. A configuration of satellite, receiver antenna, and reflective surface creating a multipath error usually requires a particular alignment [30], [31]. The GPS satellite orbits move across the sky by several minutes each orbit and those alignments would break down fairly rapidly. Also, during the 9 month period covered by the figures, at least one new satellite was added to the constellation and orbital adjustments could have been made. These event(s) would have shifted the multipath configurations at least somewhat. Given that many of the features appear to be very consistent over 30 days and several seem to be common over the entire 9 month period, multipath does not seem to provide an adequate explanation for all of the consistently repeating error components detected.

4.2 Fourier Analysis

Fourier analysis, at least as far as spectral investigations go, consists primarily of applying a transform to a data stream in the time domain, the signal amplitude, to map it to the frequency domain. This allows the identification of significant frequency components and also provides phase information. A common transform used for this purpose is the Discrete Fourier Transform (DFT) normally realized via the Fast Fourier Transform or FFT. The FFT significantly increases the computational efficiency of the transformation and may slightly reduce computational errors due to round off (by reducing the number of sequential computations performed.) There are a very large number of references discussing Fourier analysis, the DFT, and the FFT

and almost any signal analysis software package contains one or more implementations. The references listed include several volumes and papers that were used for the work described here [33], [34].

$$X(m) = \frac{1}{N}\sum_{n} x(n)e^{-i2\pi mn/N} \qquad (4.1)$$

Equation 4.1 is the generalized form of the DFT where *X* is the frequency domain representation of the time series described by *x*. Basically, the Discrete Fourier Transform generates a series of sine or cosine waves (applying Euler's formula to the exponential term in equation 4.1) with amplitude and phase calculated so that the sum of the waves is equal to the target signal. The waves have periods equal to integer fractions of the length of the signal being examined. If the signal were 100 seconds of one hertz data, the transform would use sine waves with periods of 100 seconds (1/1 of the signal length), 50 seconds (1/2), 33.3 seconds (1/3), 25 seconds (1/4), …, down to 1 second (1/100 = 1/N, the signal length) plus a bias that might be considered the 1/0 or infinite period term. For real data, such as signal intensity (or position error), the sequence of periods may be limited to ½ the number of data points (plus one) since it can be shown that the transformed values in the second half of the frequency space are just the complex conjugates of the values in the first half in reverse order. The calculated amplitude of each sine wave, suitably normalized, allows identification of the principal frequency components.

The Cooley-Tukey algorithm [33] is one of the most commonly used implementations of the FFT and was used for much of the Fourier analysis performed for this paper. The primary drawback of the Cooley-Tukey method is that in its' most

common implementation, it requires the input data to be a power of two in length. If the wavelengths of the signals of interest are not a power of two of the sampling rate, the algorithm cannot precisely align a single frequency sine wave with the signal. The signal component must be approximated by combining sine waves of other frequencies but with obviously lesser amplitudes. But the closer the wavelength is to an integer fraction of the signal length being analyzed, the less degradation of the frequency amplitude mapping will occur.

As mentioned earlier, the basis for this study was an observation by the author that there appeared to be a repeated daily pattern to the position solutions in some long term WAAS data. This periodicity has not been previously noted or reported (or was dismissed as multipath). The ideal signal length to detect such a pattern would be some number of days that equaled a power-of-two number of seconds (assuming that most of the analysis would be done on the one hertz data that was being generated by the GSV-1012 receiver in use at the time.) Since the number of seconds in a day is not power of two, a perfect solution was plainly not obtainable. Multiples of days were then considered. Twelve days equate to 1,036,800 seconds which is only 1.12% less than 2^{20} (1,048,576). So if the DFT algorithm was applied to a 1,048,576 point sequence of 1 Hz data and a daily cycle was present, there should be a significant peak at 12 cycles with only a very minor degradation in the amplitude due to the signal length not being a perfect multiple of the frequency of interest. The selected signal length should also be very close to 24 complete orbits so orbital phenomena would produce a strong peak at 24 cycles.

Alternatively, one could combine sequences of points to reduce the 86,400 seconds in a day down to some power of two by determining the mean value of the range or via some other more elaborate filtering method. The data under investigation was basically digital throughout its existence so the most likely errors were bit flips. Since such errors don't tend to be nicely distributed statistically, averaging did not seem to be the optimal solution. To smooth out any bit errors, a 200 point Hamming low-pass filter was constructed that provided 53 dB of attenuation for any periods greater than roughly 30 seconds.

Given that handling a million point array was well within the computational abilities of the computers and software available at the time, the author elected to proceed with the extraction of million point sequences from the data sources (where million is intended in the binary sense of representing 2^{20} rather than 1,000,000.)

The first data sets to be examined were the files from the OU GPS lab and the first serious problems were encountered. While this data was quite acceptable for the visualization tool, it was subject to a number of shortcomings discussed in section 3.1. Considerable time was spent examining the various data sets attempting to locate sequences of a million readings that were of sufficient quality to provide a useful baseline. Unfortunately, no such sequence could be located. In addition to the problems cited in section 3.1, there were a number of extended periods (from several minutes up to a half hour or more) where only three GPS satellites were available. (Recall that the system was still in the prototype stage while most of the OU data was collected and was not considered operational.) Since the early WAAS geo-stationary

satellites did not include an independent ranging capability, three satellites were insufficient to solve the position solution equations.

When the initial data from the Tech Center was received, it resolved almost all the continuity problems with the OU data. Software was written to provide an initial scan of the data files and extract the data into formats more palatable to Matlab, the chosen FFT analysis tool. The software generated distinct output files for the altitude, latitude, and longitude components of the errors. These files were some number of days long, usually thirteen, as the source data files were produced as twenty-four hour chunks. The output files contained two columns of data, one the actual error values and the other the error values as filtered by the low pass Hamming filter discussed previously. A summary file was also generated that included the largest gap in the input file, the total number of readings and some descriptive statistics such as minimum value, maximum value, mean, standard deviation, skewness, and kurtosis. Any gaps in the Tech Center data were filled with zeroes. No gaps long enough to affect the FFT results were detected.

In Matlab, the *importdata* feature was used to load the error files into compatible arrays. Then the *fft* function was applied, generating a million element complex array. The *abs* function was applied to the fft result array, generating an array of the magnitudes of the spectral components. Figures 4.5 thru 4.7 show the lowest frequency components of the altitude, latitude, and longitude errors for Washington, D.C., Kansas City, Missouri, and Seattle, Washington. Tables 4.1 thru 4.3 list the numerical data that produced the figures.

Because of Matlab's data indexing, the peaks at 13 and 25 actually represent 12 and 24 repetitions during the measurement period of 12.13 days (2^{20} seconds). While there is considerable variation in both absolute and relative magnitude, one or both, usually both, of these peaks is present in every sample. The peak values are highlighted in yellow in the tables.

There is frequently also a peak at 36 repetitions, although it is generally weaker than the 12 or 24 repetition peaks. A possible explanation for this peak, which does not correspond to any known physical phenomena, is a heterodyning phenomenon between the orbital and daily period errors. Heterodyning occurs when two signals are combined in a non-linear system and there is almost nothing in the WAAS position solution mathematics that could be considered linear. If heterodyning is present, it also rules out the possibility of the orbital period events being a harmonic of the daily period events. This was considered unlikely since the orbital period magnitudes are frequently larger than the daily period spectral components (which translates to a harmonic component being larger than the primary) but the heterodyning does provide an additional argument.

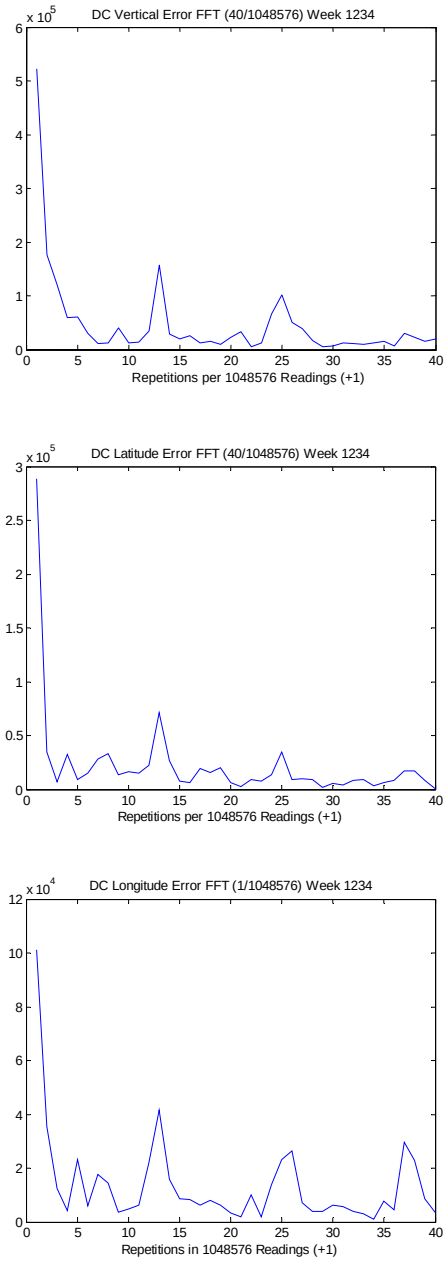

Figure 4.5 Vertical, Latitude, and Longitude FFT Results for Washington, D.C.

Table 4.1 Numerical FFT Results for Washington, D.C.

Spectral Component Magnitudes DC - Week 1234		
Altitude	Latitude	Longitude
522520	287900	101160
176120	34970	35550
120800	7020	12270
59720	32740	4230
61300	9220	23250
29850	15130	6060
11030	27940	17610
12890	32950	14330
39830	13660	3540
12800	16470	4910
13860	15010	6200
33820	22200	21960
156870	70860	41620
28930	26470	15850
19410	7510	8510
25630	6380	8270
13050	19040	6340
15120	15690	8100
8830	20400	6390
22260	6190	3240
32950	2880	2030
4530	9050	10020
12410	7310	2000
67130	13670	13860
100860	34510	23310
50050	8890	26470
38010	9610	7250
17270	9330	3830
5830	2100	3910
6270	5360	6270
12250	4210	5750
11670	8150	4040
8980	9340	3120
12320	3280	1100
14770	5970	7750
6420	8650	4630
29390	16880	29730
23210	16870	22870
15490	8760	8760
19950	450	3360
8320	2800	5390

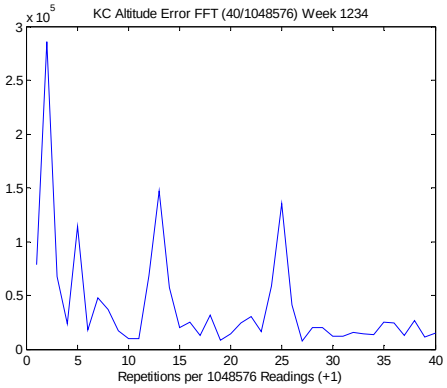

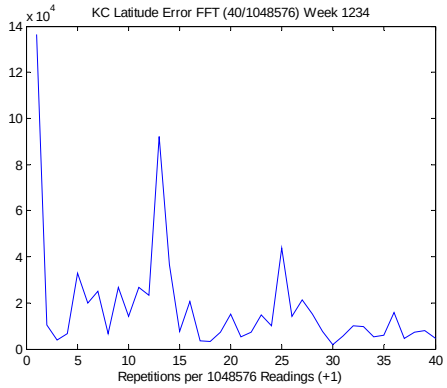

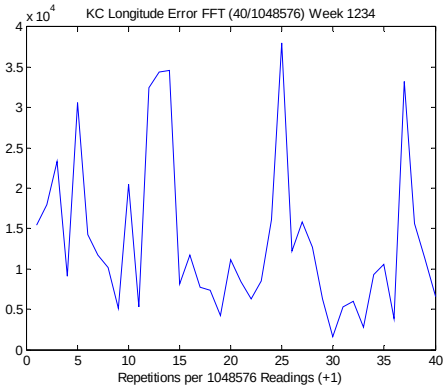

Figure 4.6 Vertical, Latitude, and Longitude FFT Results for Kansas City

Table 4.2 Numerical FFT Results for Kansas City

Spectral Component Magnitudes Kansas City - Week 1234		
Altitude	Latitude	Longitude
78680	136480	15411
285580	10420	17922
67550	3920	23322
23660	6710	9139
113930	32710	30587
18250	20030	14242
47620	24960	11763
36570	6690	10183
17210	26750	5146
9700	14280	20478
9940	26870	5275
68220	23310	32449
146960	92090	34372
57370	36590	34576
20130	7710	8121
25110	20620	11693
12750	3450	7765
31950	3310	7373
8590	7350	4281
13990	15090	11173
24090	5450	8443
30200	7420	6294
16090	14780	8476
58980	9970	16145
135240	43760	37977
40950	14270	12249
7610	21260	15770
20090	15250	12673
20260	7580	6321
11870	1940	1645
11950	5500	5294
15840	10190	6014
14570	9670	2819
13400	5270	9341
25510	5810	10550
24360	15690	3839
12800	4530	33202
26910	7490	15624
11260	8040	11330
14980	4770	6588
5440	3970	3109

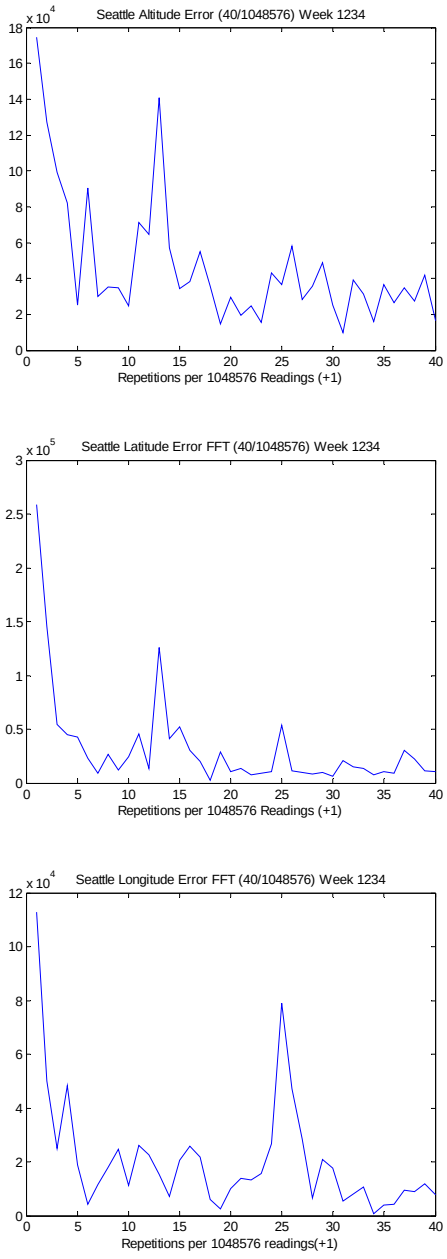

Figure 4.7 Vertical, Latitude, and Longitude FFT Results for Seattle

Table 4.3 Numerical FFT Results for Seattle

Spectral Component Magnitudes Seattle - Week 1234		
Altitude	Latitude	Longitude
174400	258640	112780
127030	145520	50070
99070	54480	24990
82140	44840	48210
25070	42530	18820
90320	23060	4290
29790	9230	11600
35330	26800	17960
34680	12030	24620
24680	24440	11170
71160	45740	25990
64580	13750	22560
140950	125940	15250
57360	41410	7130
34300	52010	20510
38290	30470	25820
54990	19860	21730
35560	2720	5910
14570	28670	2440
29750	10700	10180
19310	13370	13910
24590	7960	13290
15650	9490	15540
43350	10580	26700
36620	53570	78910
58170	11150	47060
28110	9530	28450
35600	8620	6660
49030	9660	20780
25020	6010	17660
9900	20500	5420
39410	14620	8020
31440	13520	10570
16160	7870	820
36720	10510	3890
26310	9090	4160
34890	30160	9430
27510	22230	8920
41850	11580	11950
16550	10470	7690
36510	11220	4540

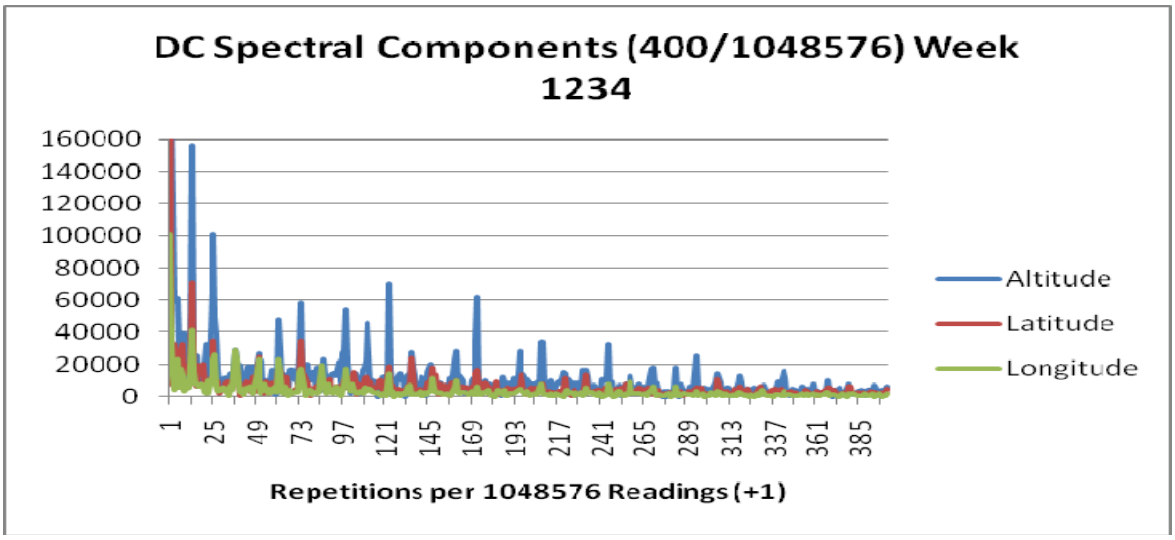

Figure 4.8

There were frequently significant spectral components at higher frequencies as shown in Figure 4.8. These were not consistent across sites and times and were generally smaller in magnitude than the orbital and daily components. Given that the satellites at the time were equally spaced around the orbital planes, it is possible to show that a perturbation due to a satellite being at a particular location in space (such as a multipath situation) could drive effects that were multiples of orbital frequencies.

It is also possible that some peaks represent harmonics of more significant components but the spacings and relative magnitudes do not readily support this option. A higher amplitude component is frequently found at a higher frequency and some of the sequences have holes in them.

Still another explanation is that at least some of the principal disturbances composing the orbital and daily errors are short duration phenomenon. A regularly repeating impulse with a little structure will produce very similar Fourier transforms. In terms of explaining such phenomena, both multipath events and the transition from

daylight ionosphere to nighttime ionosphere could produce such effects. This possibility will be further discussed in the Wavelet Analysis section.

Given the inconsistence of the higher frequency components, the remainder of this investigation will focus primarily on the orbital (11 hour 58 minute) and daily (24 hour) spectral components. The data addressed will also continue to include the 8 hour period component.

The initial set of Tech Center data provided support for the idea that the daily and orbital components of the WAAS error spectrum seen in Oklahoma City were distributed across the WAAS coverage area. Additional data was needed to verify the findings and attempt to identify some causal issues. Examination of the phase information associated with the magnitudes had not been fruitful. The second set of Tech Center data allowed examination of a wider distribution of error data, both geographically and chronologically.

Figures 4.9 through 4.12 are four sets of plots spaced across the year of data collection showing the low frequency components of the altitude, latitude, and longitude error FFTs at the seven locations evaluated. Figures 4.13 though 4.15 present the same data arranged to more clearly show the variations at the different locations during the course of a year. These could be due to seasonal variations in the atmosphere or ground cover around the antennas but with only a single year's data, that analysis would be premature.

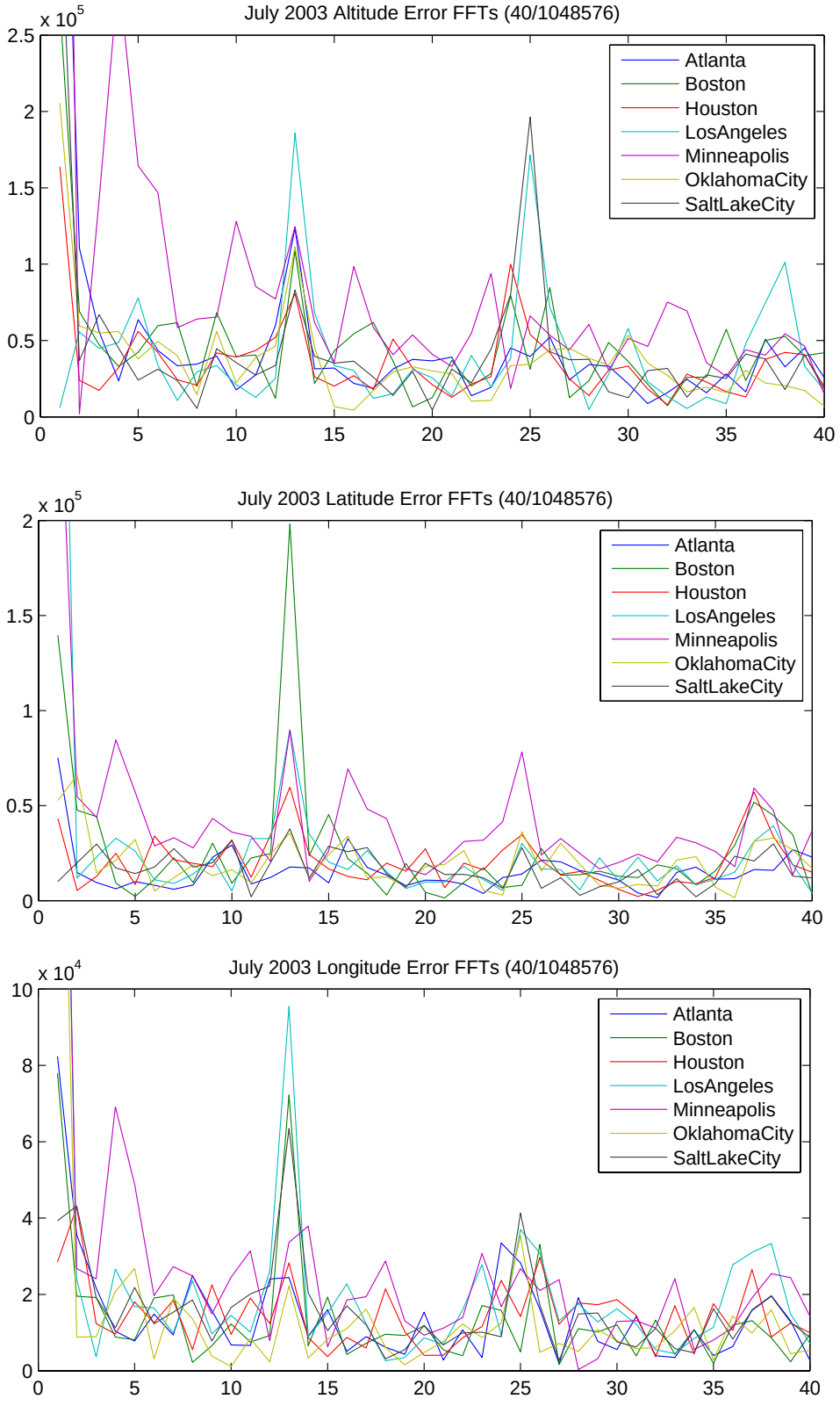

Figure 4.9 July 2003 Vertical, Latitude, and Longitude FFT Results for Seven Sites

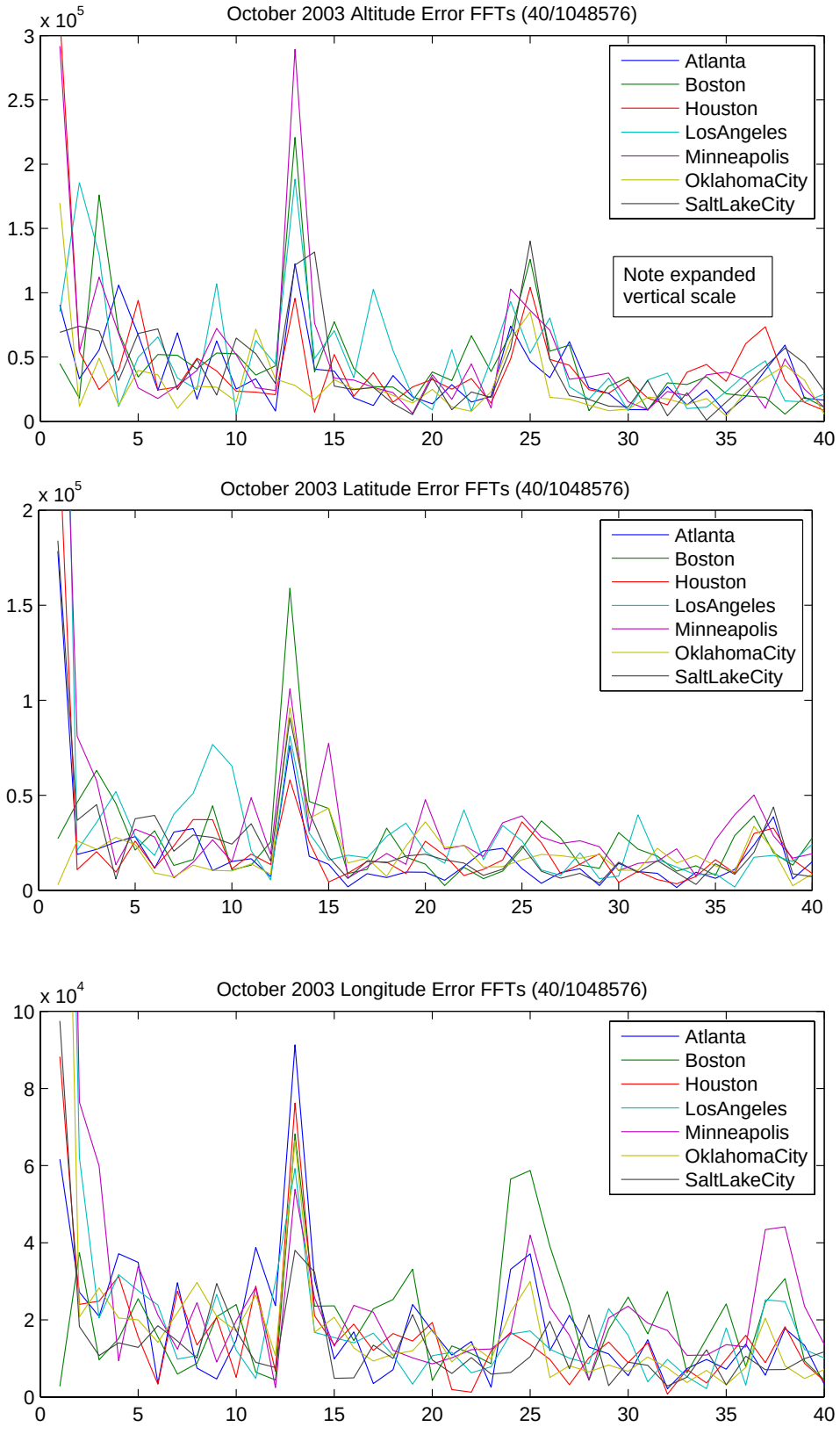

Figure 4.10 October 2003 Vertical, Latitude, and Longitude FFT Results for Seven Sites

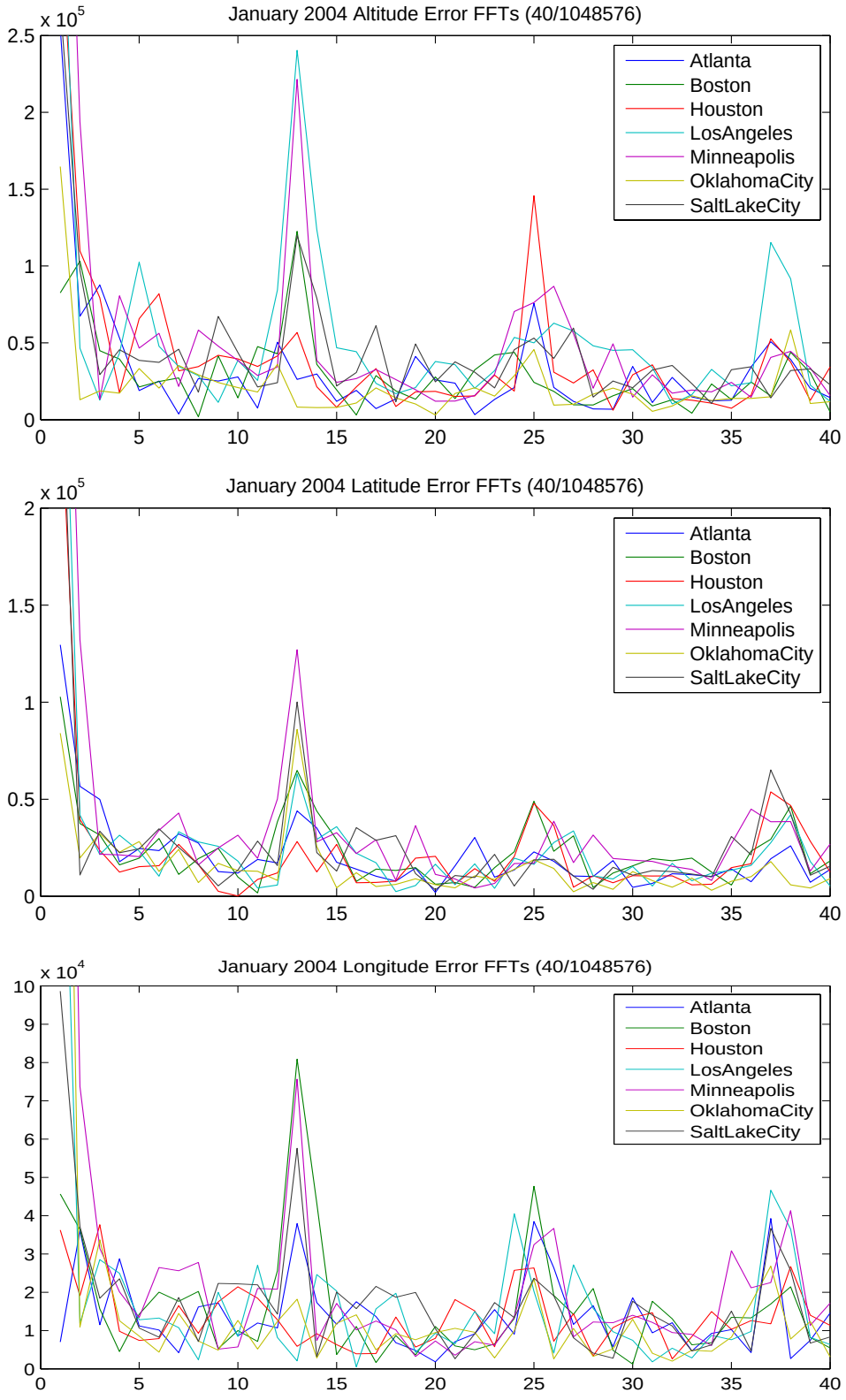

Figure 4.11 January 2004 Vertical, Latitude, and Longitude FFT Results for Seven Sites

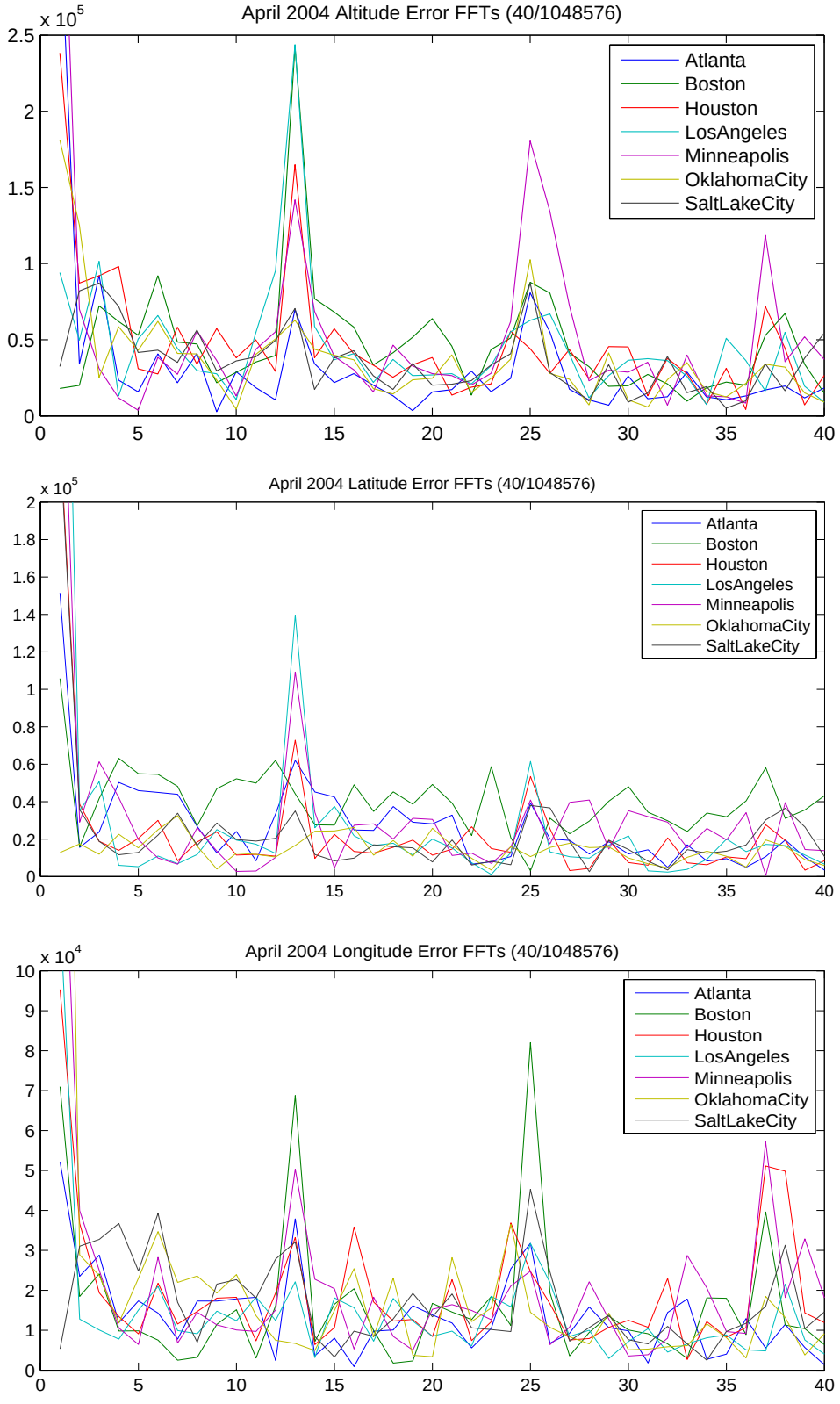

Figure 4.12 April 2004 Vertical, Latitude, and Longitude FFT Results for Seven Sites

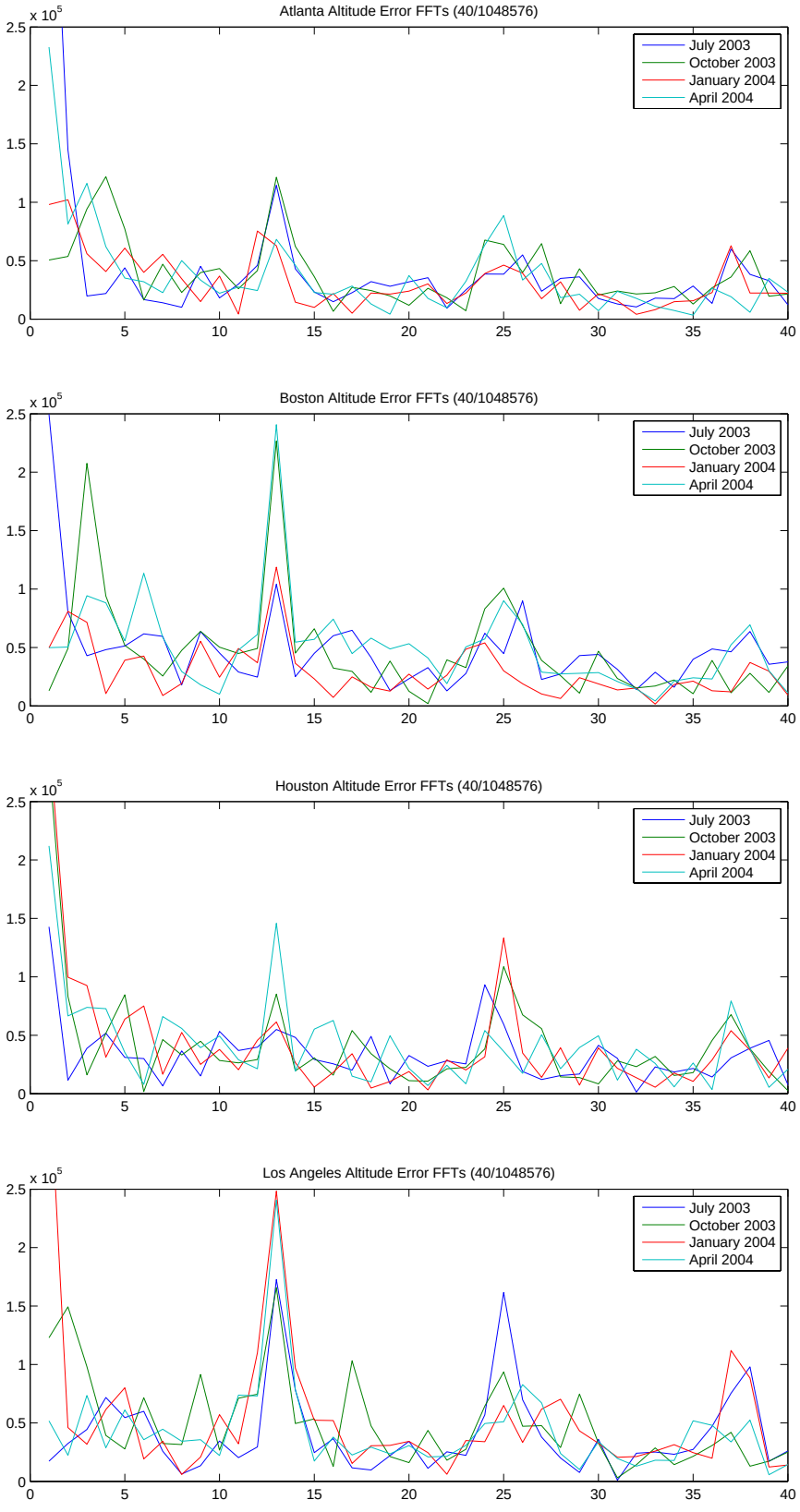

Figure 4.13a-d Vertical Error FFTs

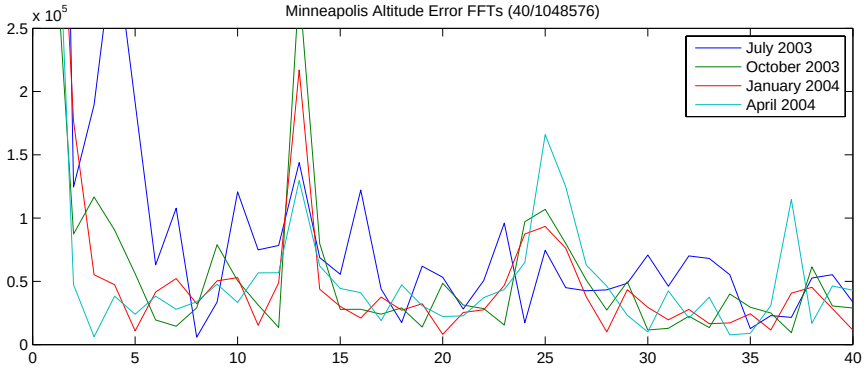

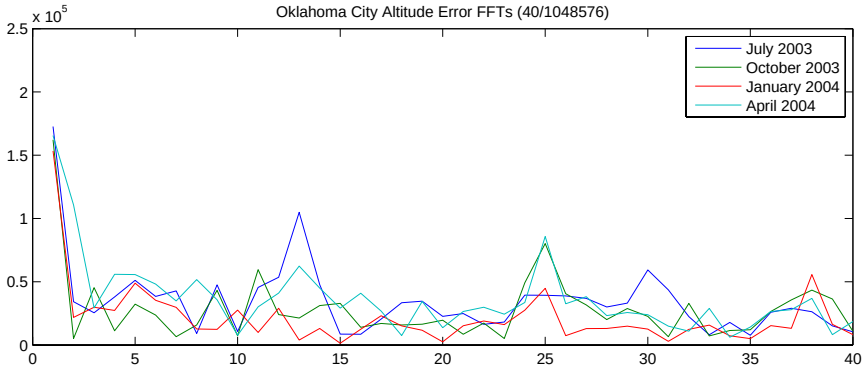

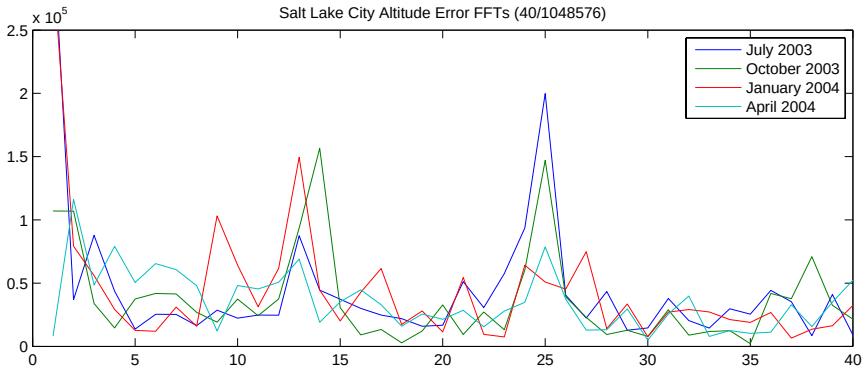

Figure 4.13e-g Vertical Error FFTs

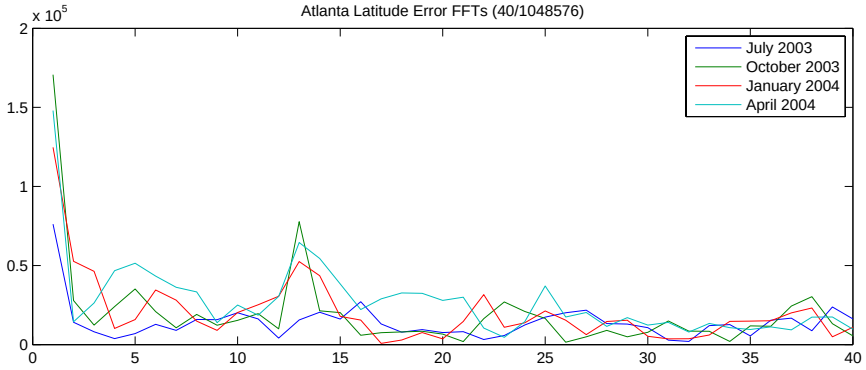

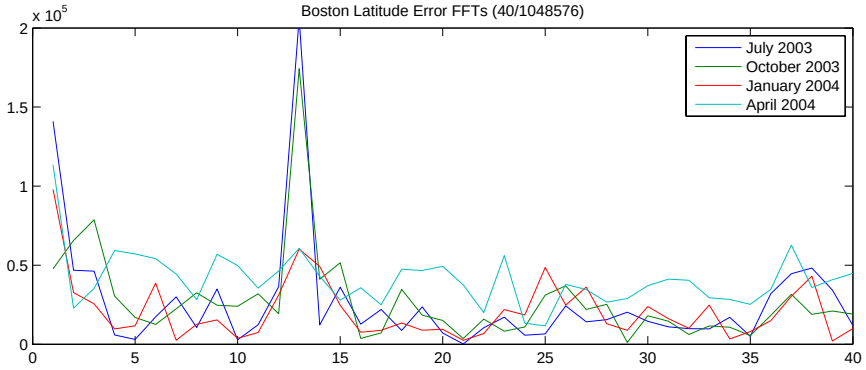

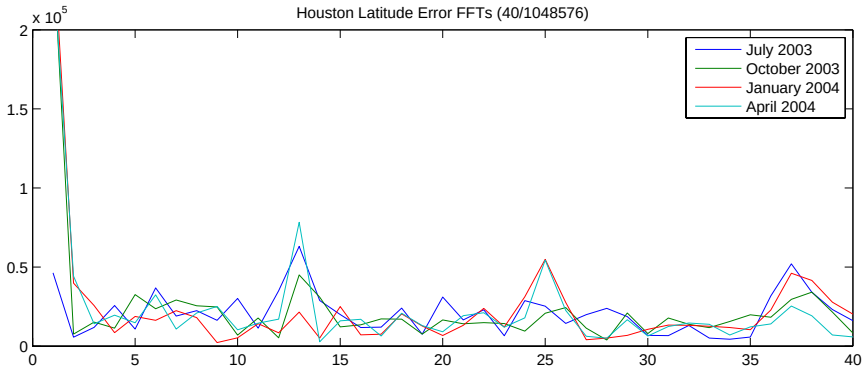

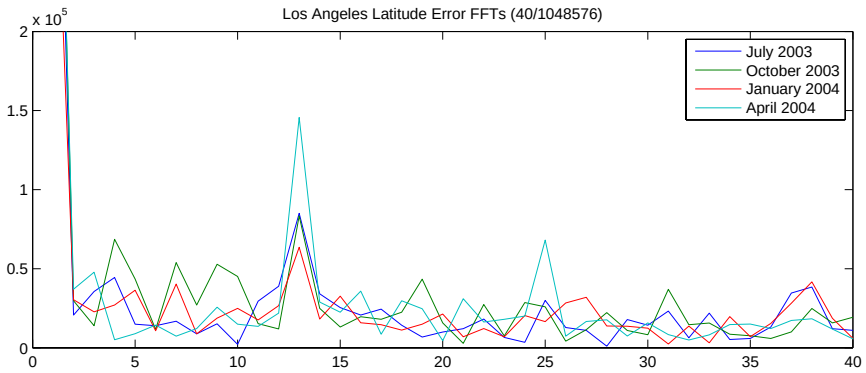

Figure 4.14a-d Latitude Error FFTs

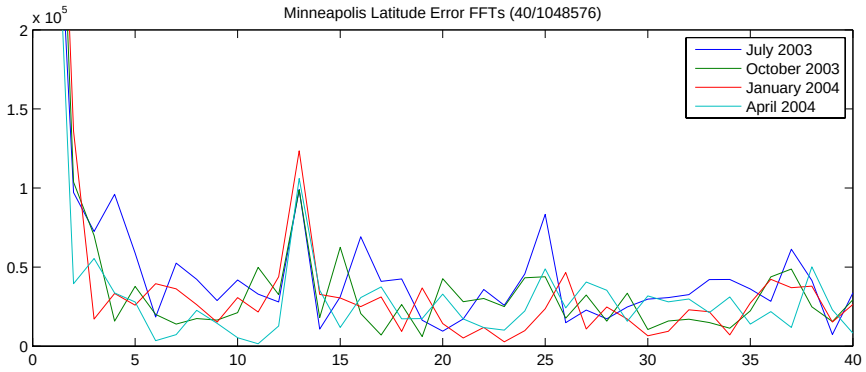

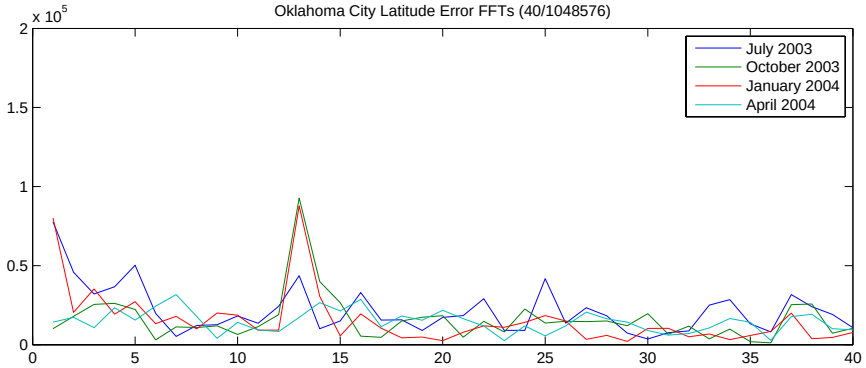

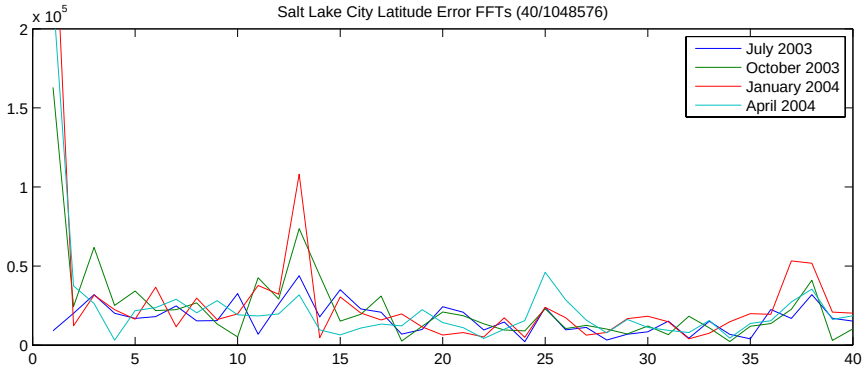

Figure 4.14e-g Latitude Error FFTs

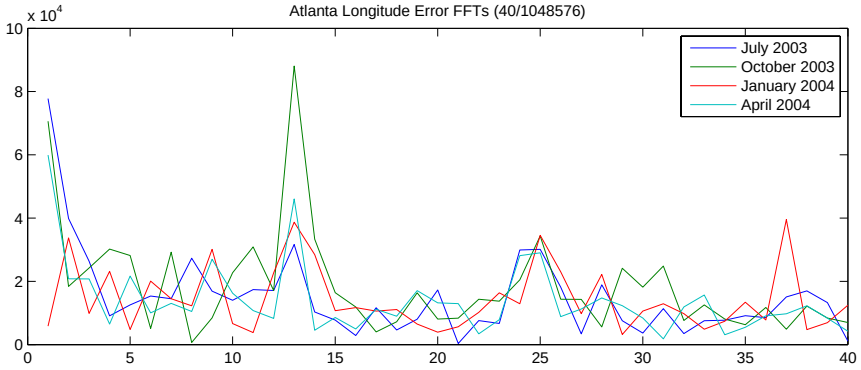

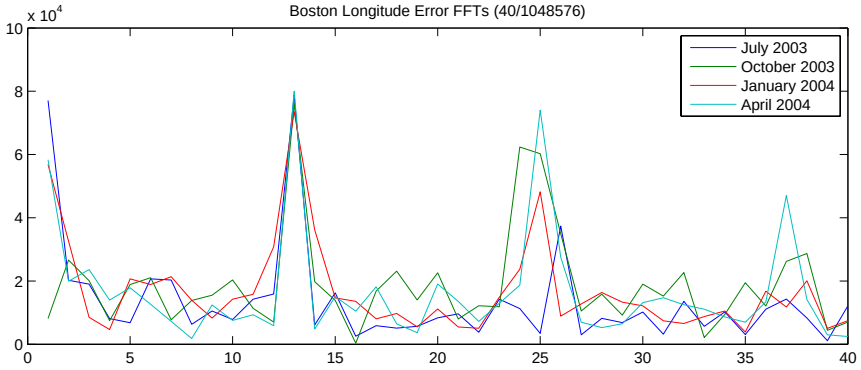

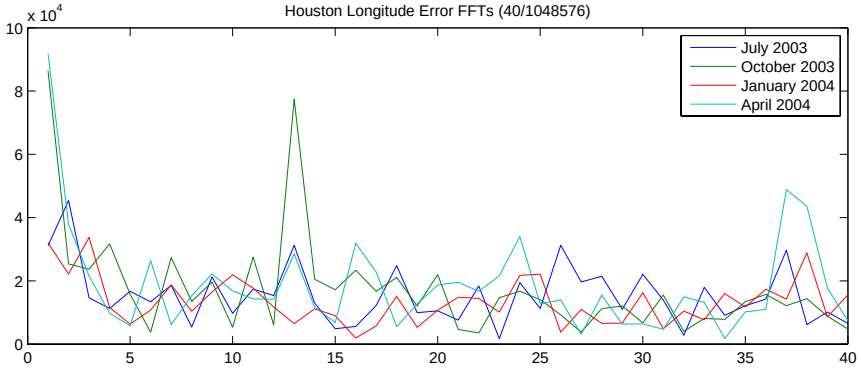

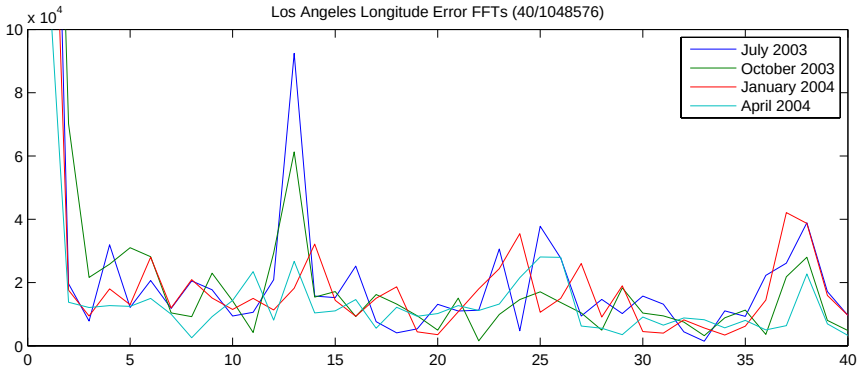

Figure 4.15a-d Longitude Error FFTs

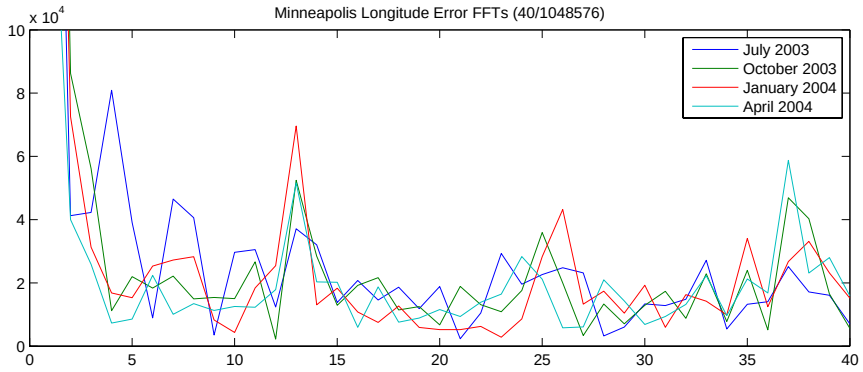

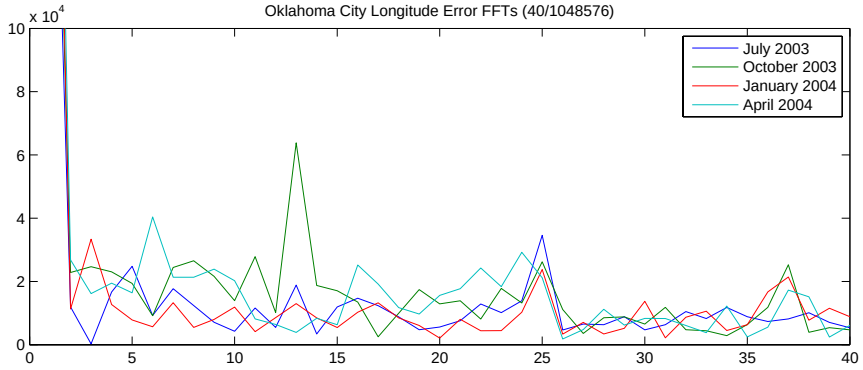

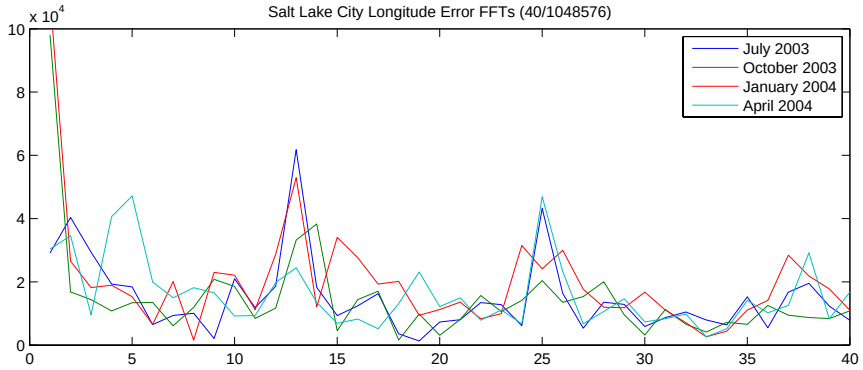

Figure 4.15e-g Longitude Error FFTs

There are obvious significant changes in the relative magnitudes of the peaks corresponding to daily and orbital phenomena, but both peaks are generally present in all the plots and represent local maxima (that is, they are larger than the other peaks for that set of data except for the spillover from the constant component).. Note that

the vertical scaling of the different plot types reflects the expected distribution of error components. The vertical errors tend to be the largest and the latitude errors are usually larger than the longitude due in part to the orbital inclination of 55 degrees combined with the motion of the satellites.

The spread of the orbital peak (the peak at 25 in the figure that represents 24 repetitions per million points) is significantly greater than the daily peak (at 13 which is really 12). By this, it is meant that there are more relatively stronger peaks at 23 and 25 repetitions than there are at 11 and 13. There are two effects that may contribute to this spread: 1) the greater difference between an integer number of orbital cycles and the observation period than the integer number of days, and 2) the presence of the second heterodyne product at roughly the same frequency. Both of these differences should be quite small however (less than one percent) so there are probably additional phenomena involved related to whatever physical effect is creating the error. While the daily peak is obviously larger on average than the orbital peak, there are numerous cases where the opposite is true. There are even a few cases where the peak at 36, the hypothetical heterodyning product, is larger than the other two. While there are substantial variations in the amplitudes across the four observation periods and the seven observation locations, the variations are not consistent. If the October peak is stronger at one location, it may well be the weakest at another. At a few locations, one or the other of the two peaks is consistent across all four measurement periods (and presumably the intervening periods) but this is definitely not a common occurrence. The variations in the error amplitudes at the different locations also seem to lack consistency. Locations closer to the edge of the

coverage area or on the west coast, which should see the most uncorrected satellites, do not seem to necessarily have larger errors. Nor does there appear to be any pattern looking at the observation locations from North to South or East to West.

These variations have significant effects on the application of this dissertation to WAAS operations but do not diminish the fundamental hypothesis that a substantial fraction of the WAAS error is contained in a very limited set of small ranges of frequencies. Focusing efforts on reduction or elimination of errors in those ranges will have significant impacts on the overall system performance.

Figure 4.16 shows a three dimensional plot of FFT magnitude versus repetitions versus the start date of the one million seconds of data examined for the longitude errors measured at Boston during weeks 1264 through 1267. The lateral axis is the repetitions per the measurement period which maps to frequency. There are significant peaks at 13 and 25 which correspond to 12 and 24 repetitions per the million second period of measurement or the daily and orbital phenomena, respectively. There is also a clear peak at 37 that is less consistent than the other two corresponding to the hypothetical heterodyning. The depth axis corresponds to the day the million seconds begins. The slice at zero corresponds to a million point (1048576 points) FFT for the error data starting at 00:00:01 of day 1 of week 1264. The slice at one corresponds to an FFT for the error data starting at 00:00:01 of day 2 of week 1264, etc. The series terminates after 18 days as the million seconds runs until the end of the 30 day observation period. Since there are only 86,400 seconds in a day, there is obviously a considerable amount of overlap between FFTs started on

successive days but the figure does show that the peaks of interest can be fairly consistent.

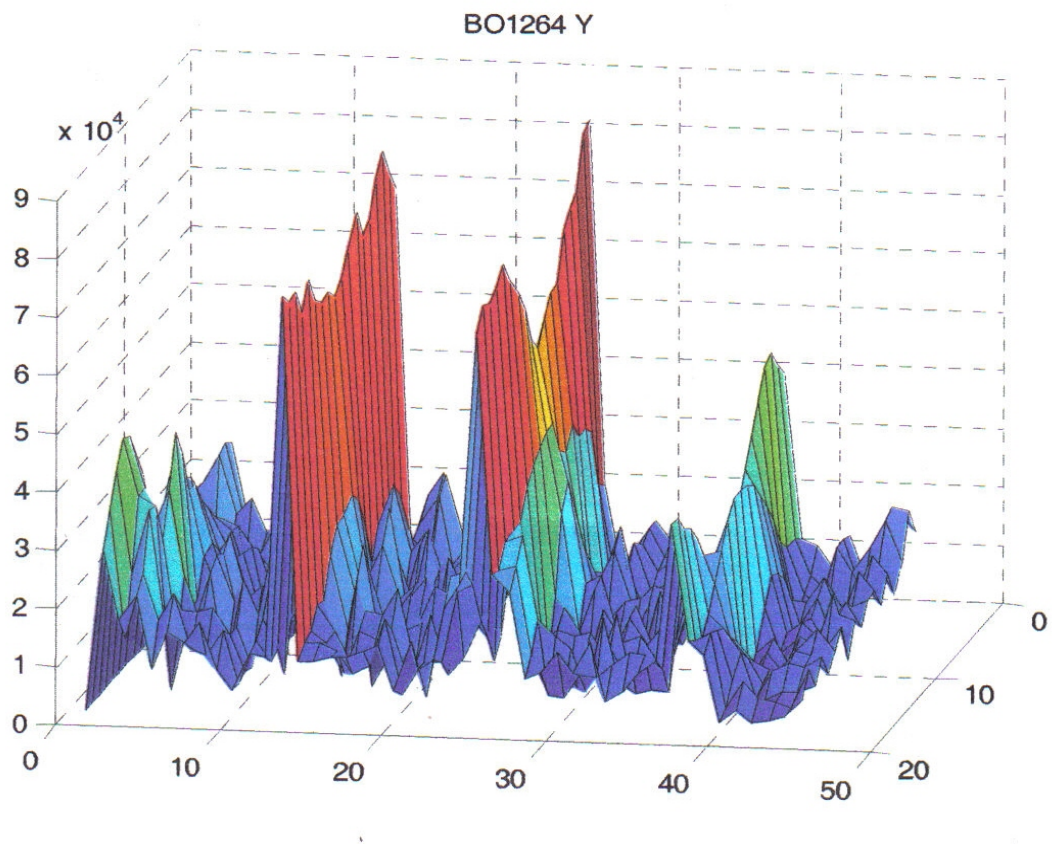

Figure 4.16 Longitude Error Million-Point FFTs from 18 Successive Days at Boston

Examination of the phase information garnered from the FFT analysis did not produce very consistent results. Files containing the phase information associated with the type of amplitude information shown in Figure 4.16 were generated for all 84 datasets (7 locations times 4 periods times 3 coordinates). This allowed examination of the phase information for daily variations over 17-18 day periods and comparison of the phases across nearly a year. As might be expected, the strongest persistent peaks had the most consistent phase results with a tendency for the angle to be

relatively constant or else monotonically (within the noise bounds of the data) increasing or decreasing. Data from most of the other peaks tends to randomly jump around. Figure 4.17 shows the FFT generated phase information for the Boston data plotted in Figure 4.16.

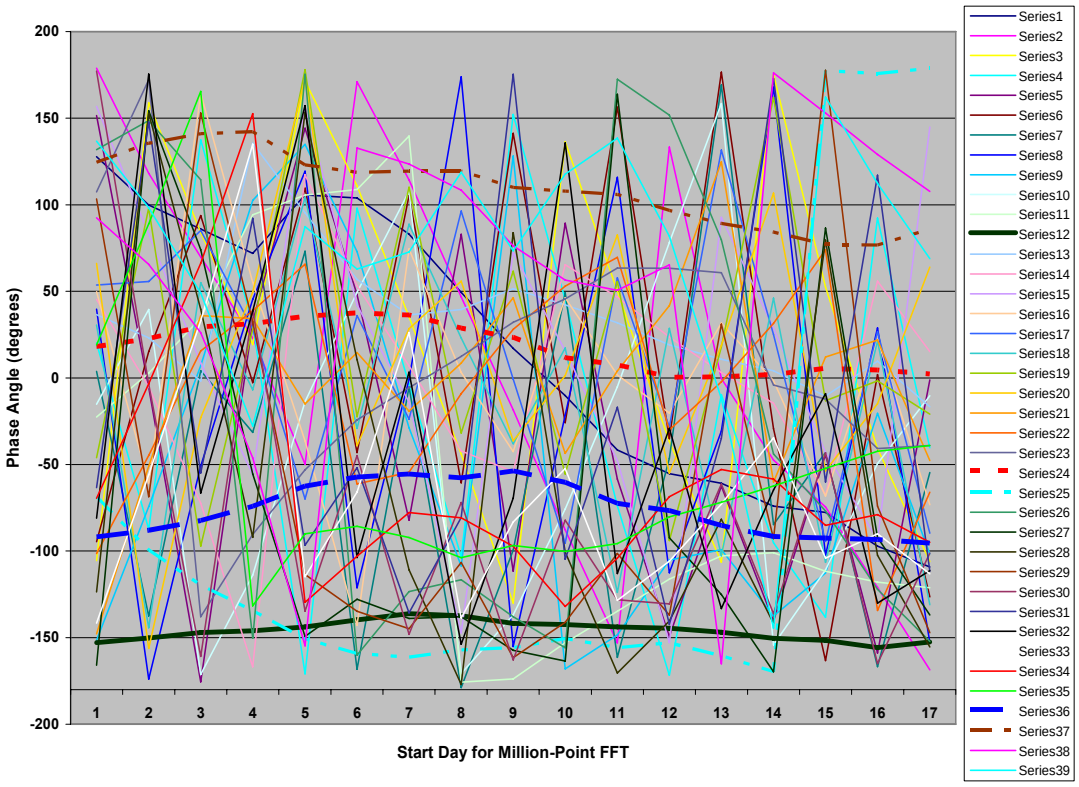

Figure 4.17 Phase Angle for Lowest Frequency Components – Boston Longitude Error FFT, GPS Week 1264-1267

In the figure, the principal components of interest are highlighted. The "Series" number in the legend corresponds to the number of repetitions in the observation period so that "Series 12" represents the once-per-day effect and "Series 24" the orbital. It was fairly common for one or both of the peaks adjacent to the strongest peaks to also have relatively smooth phase information, which is why series 25 and 37 are also highlighted. The remaining components appear highly randomized.

Figure 4.18 through 4.23 show plots of the phase angle versus "start day" of the FFTs for Los Angeles altitude errors and Boston latitude errors, respectively. (Note that the transition from -180 to +180 in the Series 36 data in Figure 4.18 is due to wraparound and is not an actual 360 degree phase shift.)

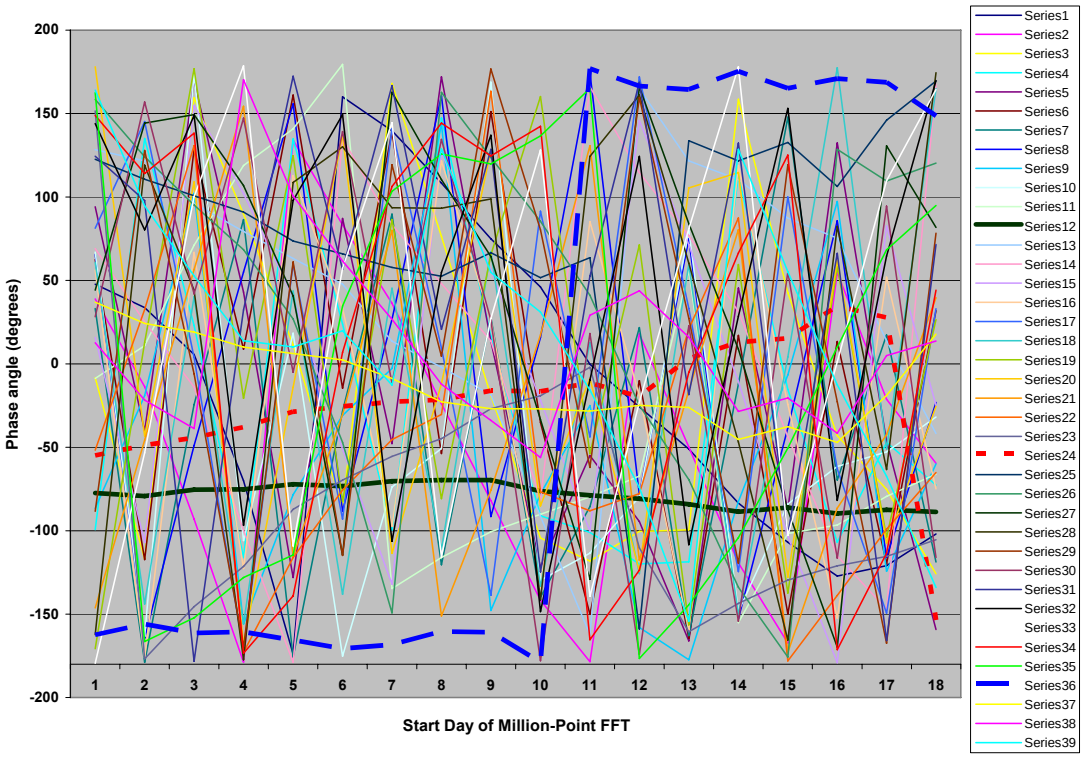

Figure 4.18 Phase Angle for Lowest Frequency Components – Los Angeles Altitude Error FFT, GPS Week 1226-1229

The October 2003 data is not included in these figures because the data sets were truncated to 18 days (versus 30 or 31 for the other three periods) due to a system problem. This limited the number of consecutive million-point FFTs that could be generated to five which did not generate sufficient trend information to be useful.

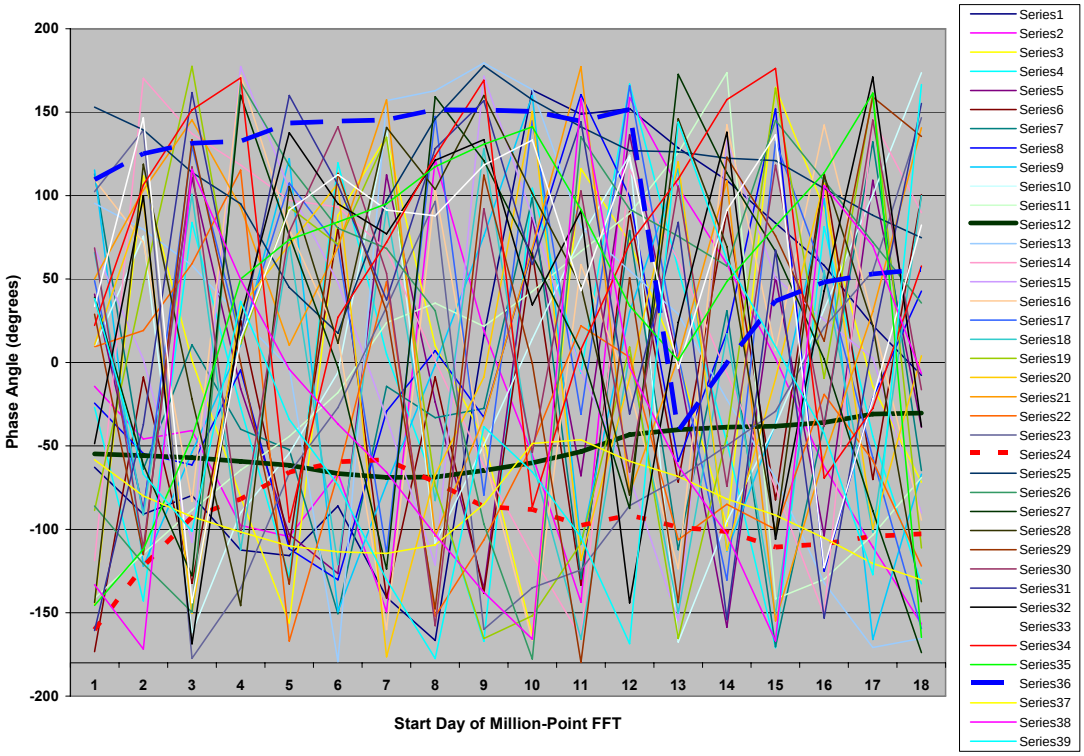

Figure 4.19 Phase Angle for Lowest Frequency Components – Los Angeles Altitude Error FFT, GPS Week 1251-1254

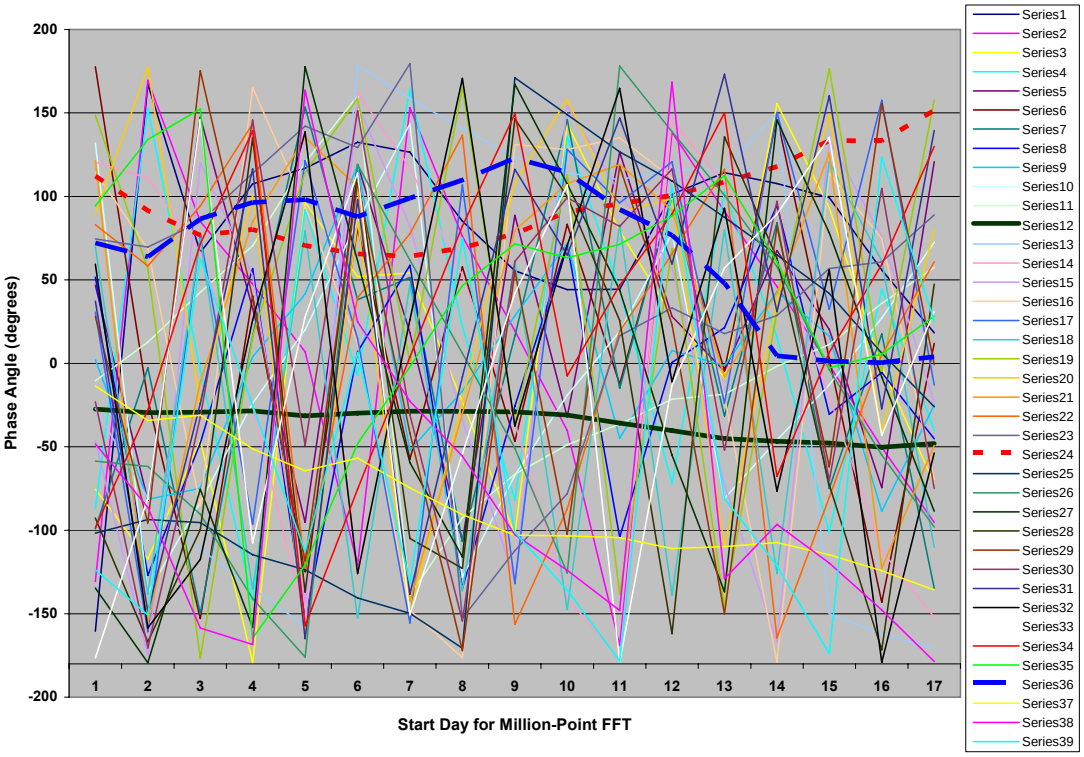

Figure 4.20 Phase Angle for Lowest Frequency Components – Los Angeles Altitude Error FFT, GPS Week 1264-1267

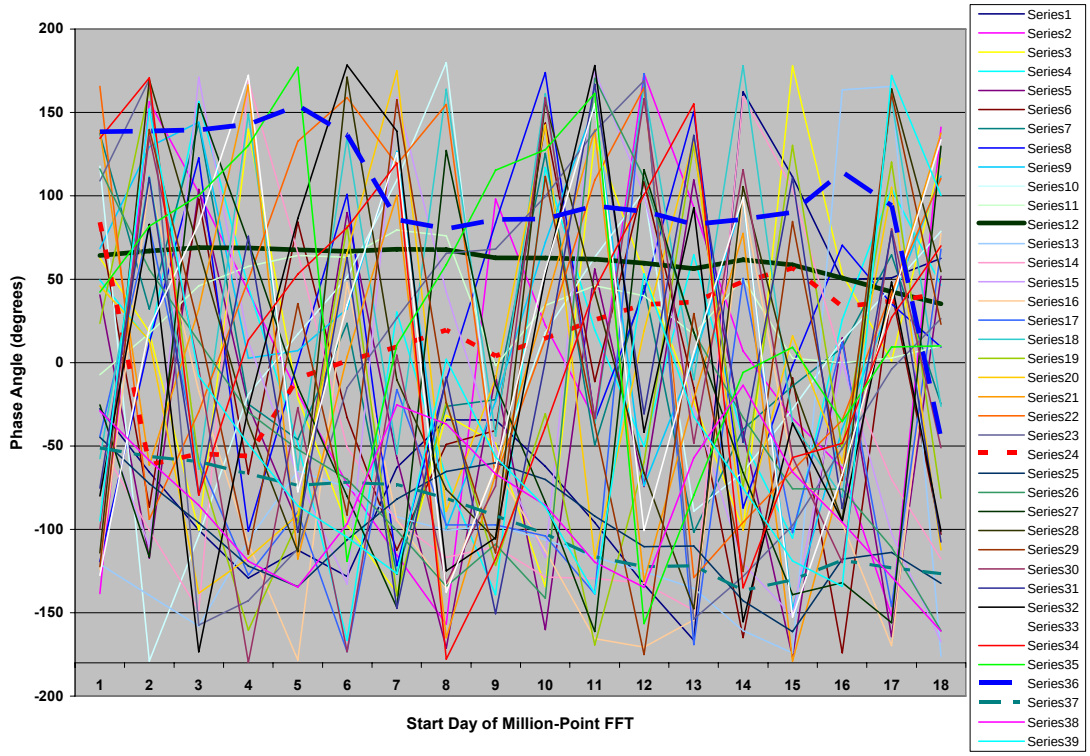

Figure 4.21 Phase Angle for Lowest Frequency Components – Boston Latitude Error FFT, GPS Week 1226-1229

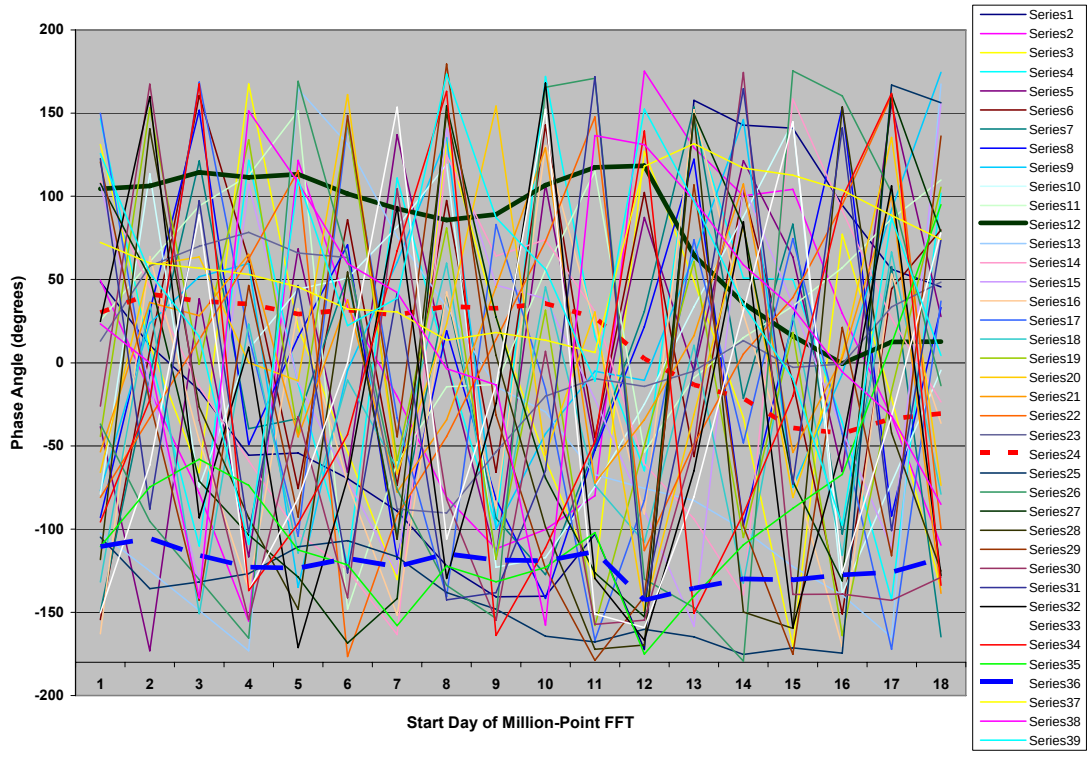

Figure 4.22 Phase Angle for Lowest Frequency Components – Boston Latitude Error FFT, GPS Week 1251-1254

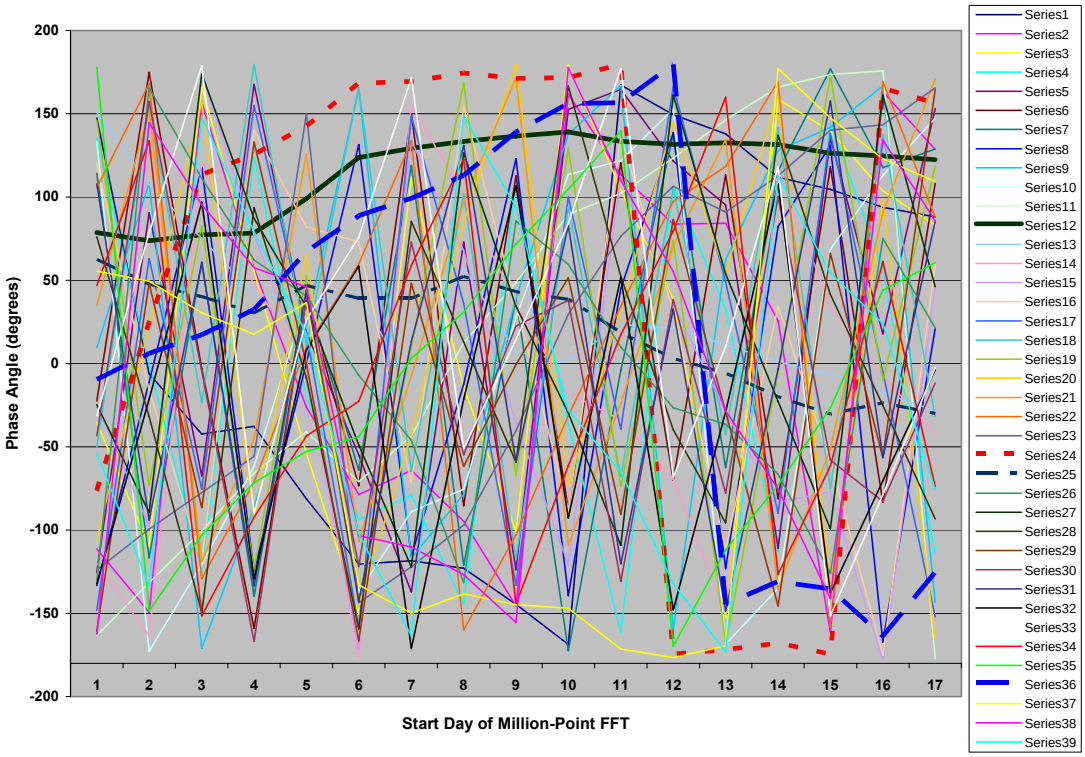

Figure 4.23 Phase Angle for Lowest Frequency Components – Boston Latitude Error FFT, GPS Week 1264-1267

The 24-hour period component's phase (the dark green solid line) is relatively constant across the Los Angeles data but shows more variation in the Boston plots. The orbital component's phase (the red dotted line) drifts across a wider range in either direction and has some significant discontinuities. The line corresponding to the eight hour period (in blue dashes) has similar but apparently unrelated variations. None of the variations correspond very well to physical phenomena such as the movement of the satellite orbits.

While the phase information provided some interesting trends, it was not consistent enough to provide any strong clues to the base causes of the signal

variations of interest. It would be beneficial to get a more continuous set of data collected over a period of at least a few years.

4.3 Wavelet Analysis

Wavelets are mathematical functions that can be used in a manner very similar to the way sines and cosines are used in Fourier analysis. The functions in question are finite in length (which translates to time for the purpose of this analysis) but can be scaled to essentially any size or translated to any point along the time line of a signal. Usually the basic form of a wavelet or "mother wavelet" is quite short so that it can be used to identify very small signal features. The simplest wavelet, the "Haar", is only two points.

Rather than focusing almost entirely on attempting to reconstruct a signal by combining functions like the Fourier analysis does, wavelet analysis allows identification of features and changes in composition of a signal as a function of time. While a Fourier analysis provides information on the spectral components of a signal, it cannot tell when those spectral components were present. Wavelet analysis allows localization of frequency components (if such localizations exist). So if there is a change in the spectral composition of a signal, wavelet analysis will allow determination of what the spectral components were before and after the change and localize when the changes occurred.

Wavelet analysis will also identify discontinuities and short term effects which are much more difficult to ascertain and may corrupt the results obtained with Fourier analysis. The Haar wavelet mentioned above, for instance, is particularly useful for identifying edge effects. Other wavelets are more useful for identifying other features.

Like Fourier analysis, there are a tremendous number of references for wavelet analysis. The reference list for this study names only a few [35], [38], [39], [40], [41]. The mathematics of wavelet analysis can get quite involved but a thorough understanding of the mathematics is not required for the relatively straightforward tasks of this study, the spectral decomposition of the WAAS error components.

During the analysis, a wavelet is set to an initial scale and then used to transform the signal of interest. At each position the correlation coefficients between the wavelet and the signal under study is determined and saved. Then the wavelet is shifted along the signal by some amount and the correlation calculation is repeated. When the end of the signal is reached, the wavelet is scaled up by some amount and the process is repeated. This continues until a maximum scale value is reached. This process may be performed as either a discrete wavelet transform (DWT) or a continuous wavelet transform (CWT). The CWT examines all scale and shift values in the range of interest. The DWT shifts and scales things by powers of two and, so, can be considerably less demanding computationally. However, since some of the components being examined by this study might be overlooked in the step from one power of two to the next, the CWT was selected.

The Matlab family of analysis routines includes a quite extensive wavelet toolbox and the *cwt* feature met the needs of this study by providing a graphical output from the continuous wavelet transform. It also allowed easy selection of the wavelet type and the limits and spacing of the analysis steps.

The wavelet analysis re-examined most of the same data used for the Fourier analysis. To limit the computational load, the original 1 hertz data was downsampled

to one reading every two minutes. This was accomplished by writing a simple Matlab macro that calculated the average value for each 120 data points and inserted it into a new array. This reduced the one million element arrays used for the FFT studies down to less than 9,000 which the *cwt* command seemed to handle without unreasonable delays. Note that the "short term" effects mentioned above are still significantly longer than two minutes so they will not be masked by the downsampling.

Following up on the possibility that some of the spectral features detected in the Fourier analysis might be due to short term effects, the Haar wavelet was applied to a number of the data sets. The Haar wavelet is just a two element sequence [1 0] and produces high correlations for edges or sharp transitions. Figures 4.24 through 4.27 show the output from the transform routine. In the figures, lighter colors represent higher correlation amplitude. Both large negative and positive correlations are lighter colors. The horizontal axis is the time scale with each point representing two minutes of data. The vertical axis represents the scaling of the wavelet, i.e. how "stretched" it is from the base wavelet.

Figure 4.24 is the Haar CWT for Washington, D.C. altitude errors and it shows that the only strong correlation (indicating an edge) occurs at about 107 hours (3200 time steps times 120 seconds per time step is 106.667 hours) into the sample and is largely independent of scale. This does not seem likely to have produced the multiple components shown in the DC FFTs shown in Figure 4.5. Later figures using other wavelets suggest longer term phenomena are present. Figure 4.25 is the Haar CWT for the DC longitude errors and shows a different area of high correlation at about 43 hours into the sequence. Plots of data from Kansas City (Figure 4.26) and Seattle

(Figure 4.27) show more consistent features in terms of repeated edge type effects but at lower correlation values than seen in the DC data.

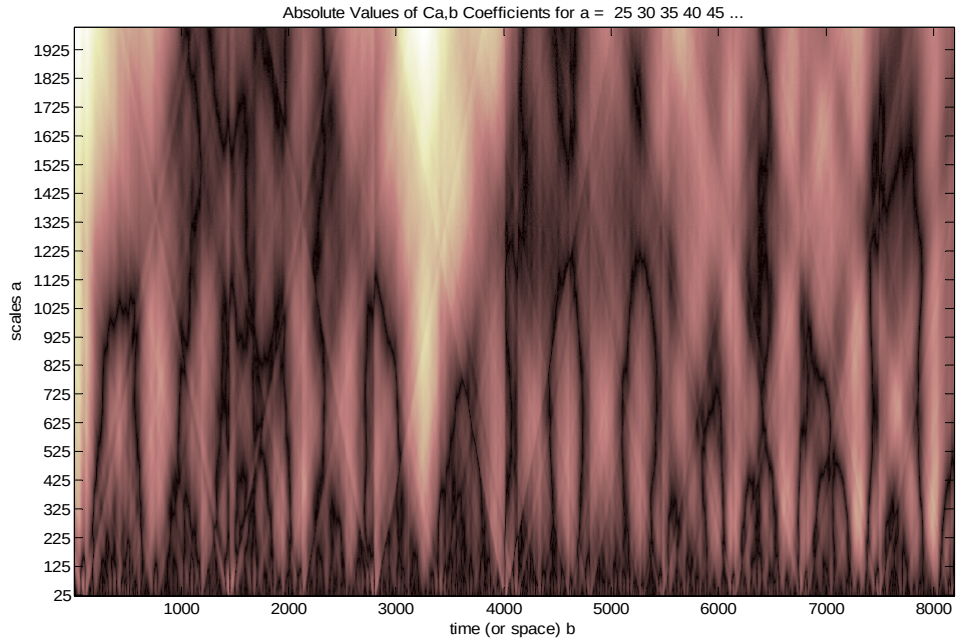

Figure 4.24 Haar CWT of DC Altitude Errors from Week 1234

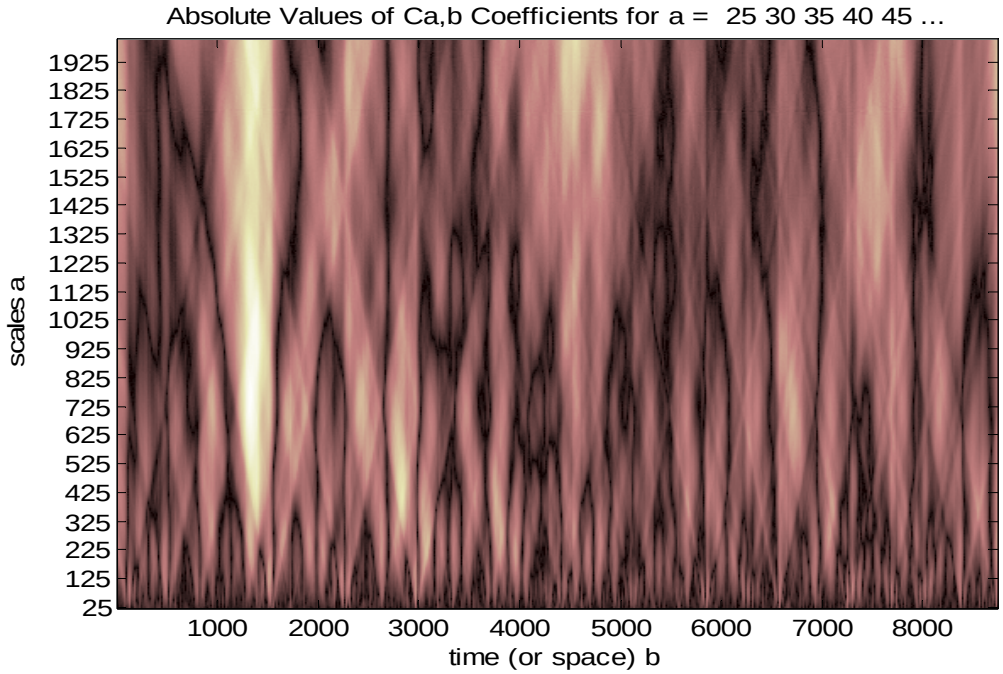

Figure 4.25 Haar CWT of DC Longitude Errors from Week 1234

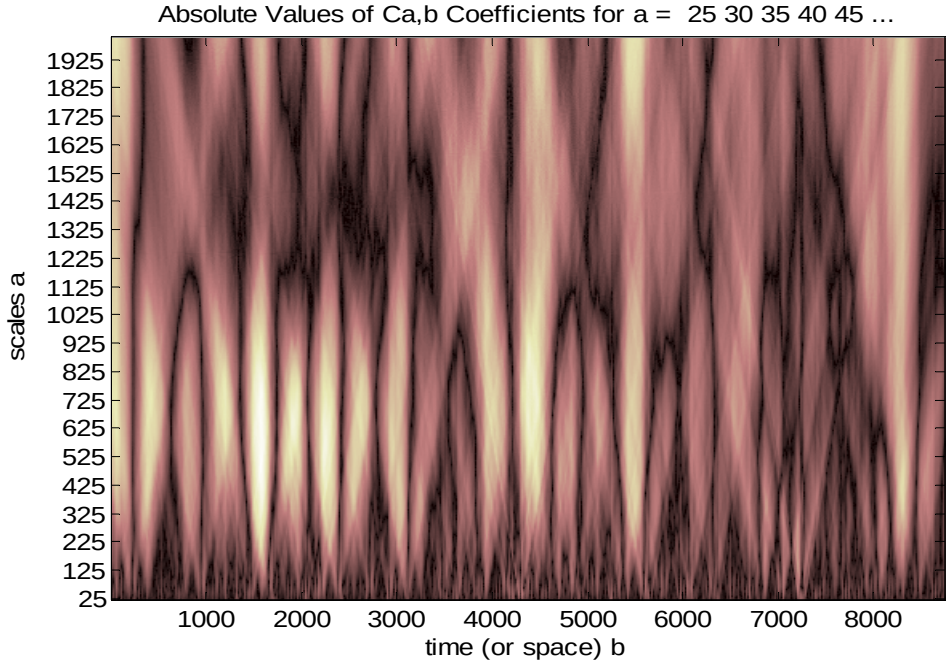

Figure 4.26 Haar CWT of KC Latitude Errors from Week 1234

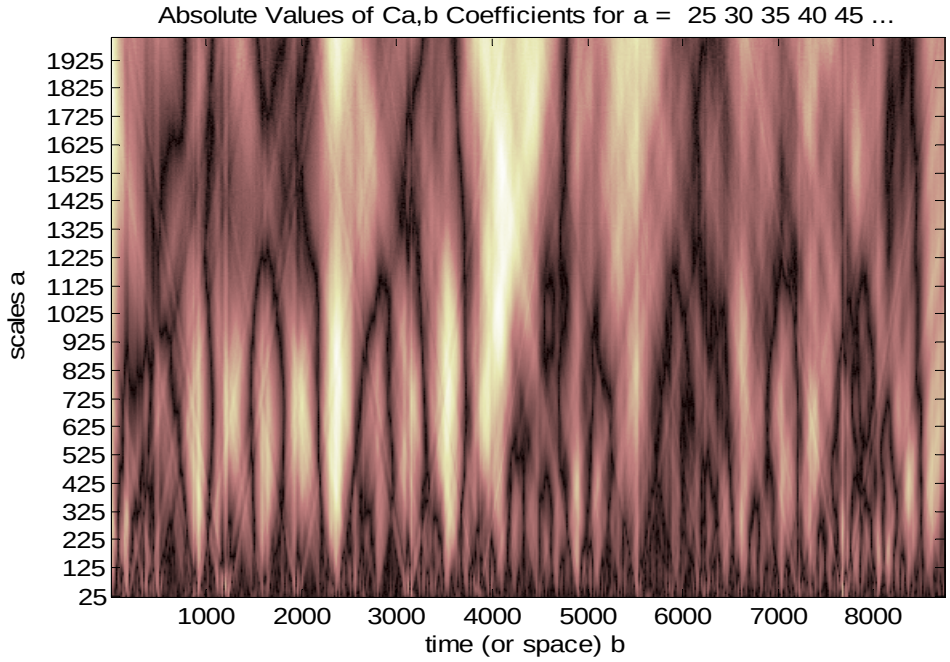

Figure 4.27 Haar CWT of Seattle Altitude Errors from Week 1234

The second transform considered is actually a family of wavelets of increasing complexity that are also considered useful for detecting edge effects and particularly

signals that are polynomial in nature but also have some sinusoidal characteristics. The Daubechies wavelets for Db4 and Db12 are shown in Figures 4.28 and 4.29.

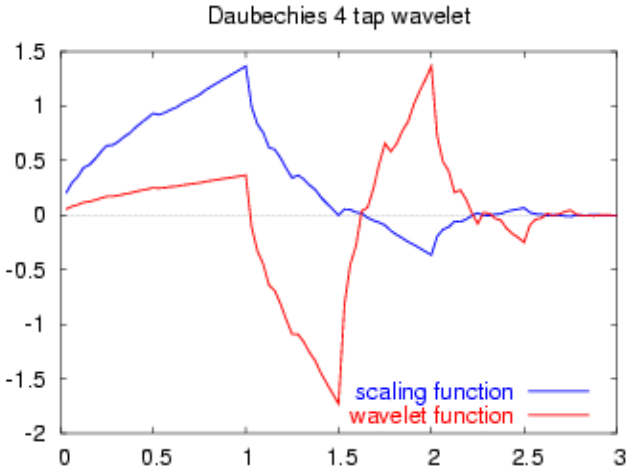

Figure 4.28

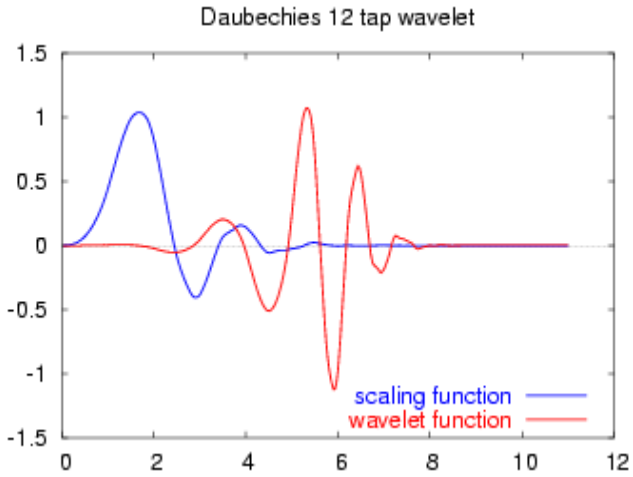

Figure 4.29

The scaling functions included in the figures relate to the mathematical treatment of wavelets and are not essential to this discussion. Also note that the naming convention for Daubechies is not universally consistent so a Db4 in one reference may correspond to a Db2 or a Db16 in another.

Figures 4.30 and 4.31 are Daubechies CWT outputs for the same Seattle altitude error data. Definite structures (cyclical variations in correlation intensity) are visible. Each dark area represents a zone of very low correlation. If it is assumed that the position error as a function of time has a distribution similar to a sinusoidal (rather than a repeating impulse) and view the Daubechies-4 as one period of that sinusoid (with low amplitude tails), then the correlation of the Daubechies as it is translated along the signal should show two minima for each cycle of the error signal (basically where it is 90 degrees out of alignment and 270 degrees out of alignment.) A strong correlation, indicated by lighter coloring, across the width of the figure would indicate a consistent waveform present for the entire period of observation.

If the daily error component is present, there should be about 12 repetitions in the 1,048,576 second observation period which has been downsampled to an 8,738 element sample. From the 12 repetitions, there would be 24 zones of low correlation. Dividing the number of elements by the number of repetitions times the length of the wavelet should produce a good estimate of the scale for that area of the spectrum for a wavelet that represents one cycle or period of the noise signal. More complex wavelets include multiple cycles and require adjustments to this calculation. Assuming the Db4 wavelet is a one cycle representation, the result of that division is 243. Examining the figure, the number of dark zones crossed when the scale is 243 is higher than predicted, more like 48 or 50 depending upon how you count some of the dark zones in the transition zones. But closer examination of the Db4 wavelet shows that only about half of the wavelet function is sinusoidal (the section from about 1 to 2.5 in Figure 4.28). The leading and trailing sections of the wavelet contribute little to

the correlation value, so a more realistic scale factor would be around 500 to 525. In that range of scale factors, the count of dark zones is 24 and, for most of the range, there is very high correlation. Applying this logic to the orbital period phenomena, 48 dark zones is the number of minima that should be expected for the 243 scale.

Also of interest is the extensive area of even higher scale (hence lower frequency) which suggests spectral components at 4 or 5 repetitions per 12 days. Peaks in this area were routinely, but not consistently seen in the FFT plots and were assumed to be spillover from the offset, or DC component, of the signal since there are no obvious physical phenomena to explain perturbations with periods of several days.

The Db8 transform applied to the same Seattle altitude data produced very similar results. The Db8 function includes a little over two complete cycles but is over twice as long so the scaling produces very similar results. The wavelet does appear to produce sharper results at the lower scale factors, corresponding to higher frequency components.

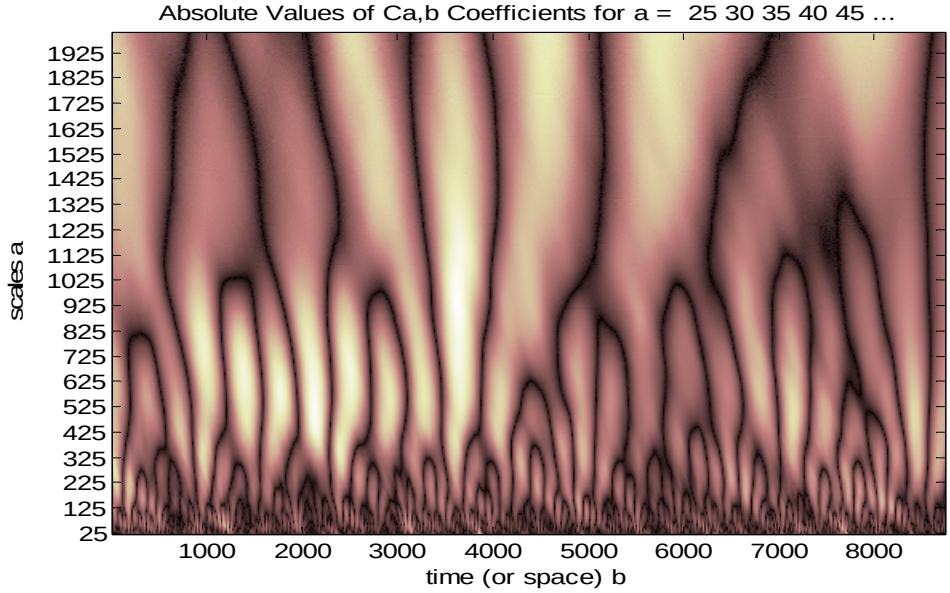

Figure 4.30. Db4 CWT for Seattle Altitude Error

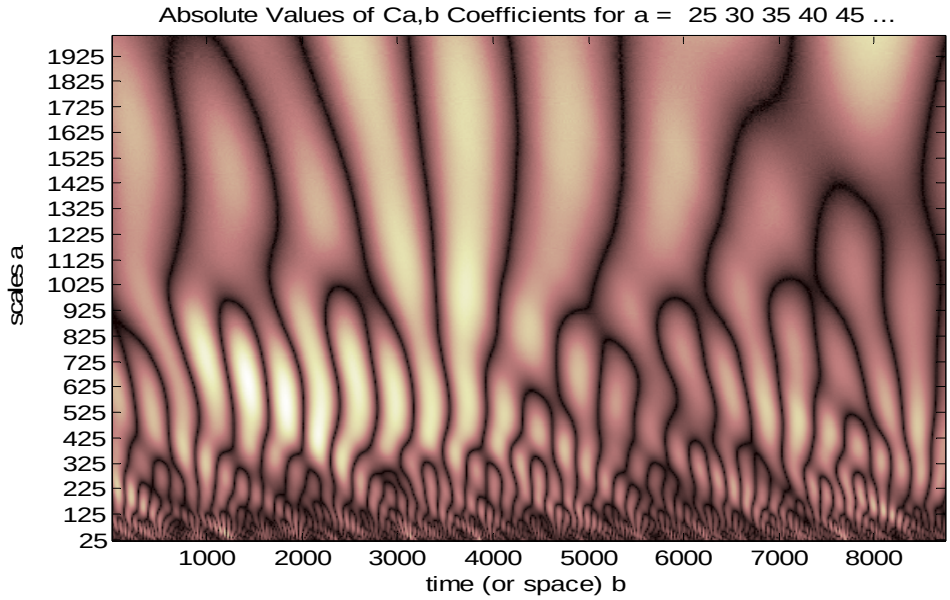

Figure 4.31. Db8 CWT for Seattle Altitude Error

While the consistency of spacing (which corresponds to the period of the error cycle) is not perfect, the variation is not very large. This strongly supports a regular phenomena rather than a random one.

The third wavelet type examined produced some of the best results. The Morlet wavelet resembles a sinusoid overlaid by a Gaussian distribution. The wavelet contains about three cycles in a base length of four. Recalculating the scale factor for the 24 hour cycles predicts a value of 546. Figure 4.32 is the same CWT output as shown in Figures 4.30 and 4.31.

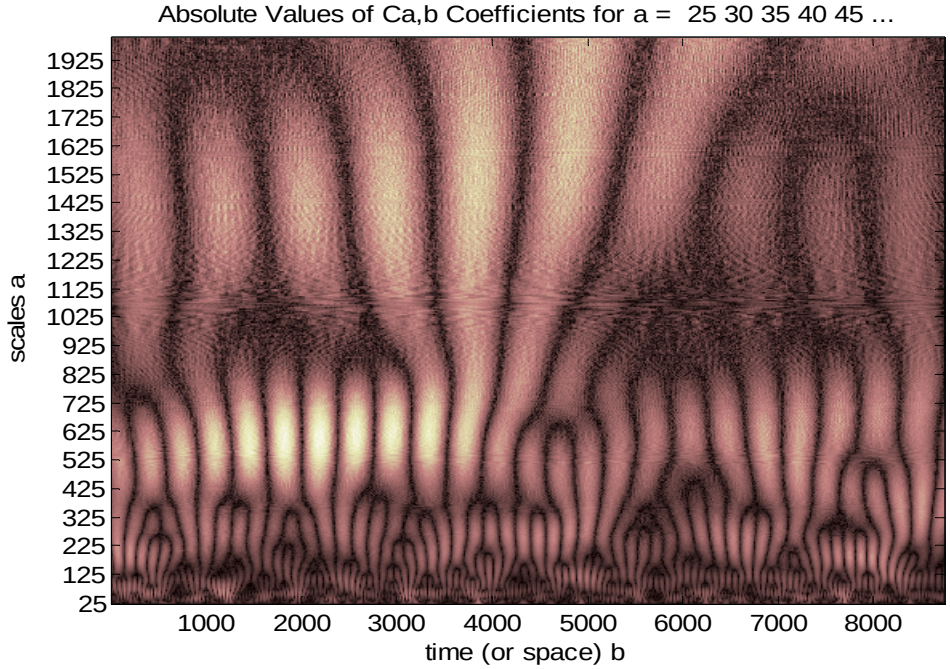

Figure 4.32. Morlet CWT for Seattle Altitude Error

By zooming in on the lower scale (higher frequency components) and reducing the step size to the minimum, an even clearer picture is produced in Figure 4.33. The two lines show scale regions that have 24 (at scale equal to 541) and ~48 (depending upon how the branching at time 5700 and 7800 are counted – at scale equal to about 275). This is in very good agreement with the calculated scale factor and once again the spacing regularity is very good at these scales.

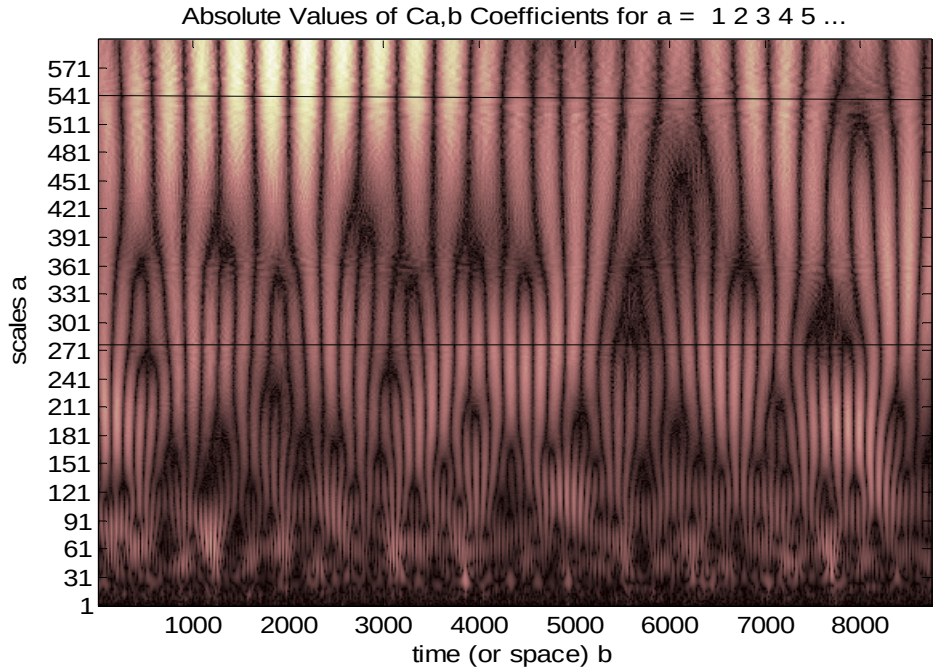

Figure 4.33. Morlet CWT for Seattle Altitude Error - 2

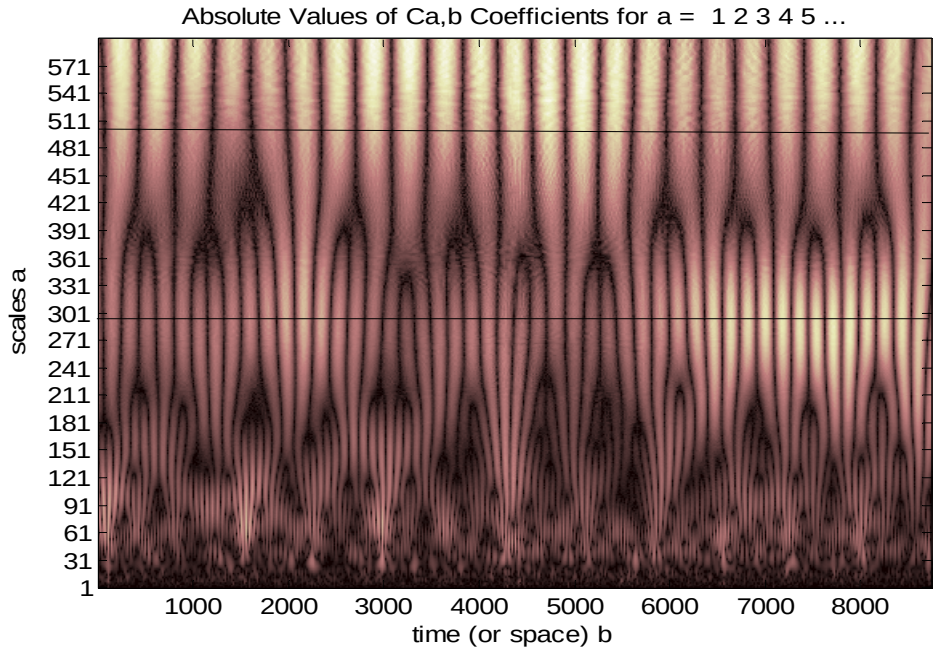

Figure 4.34 Morlet CWT for DC Altitude Error

Figure 4.34 is the CWT of the DC altitude data and shows less motion along the scale axes where the transition branchings occur. The uniformity of spacing of the

dark zones strongly supports a steady sinusoidal function and should allow for at least some phase analysis work.

The continued branching at the lower scale values indicates that higher frequency components are present. They could be more easily identified by a lesser downsampling and probably a shorter observation period.

The results presented here are fairly representative of all the data examined. Additional Morlet CWTs of a sampling of the other data sets are provided in Figures 4.35 through 4.44. The results clearly show that spectral components of the WAAS errors corresponding to orbital and daily phenomena in all three dimensions have significant correlation with wavelet functions that are at least somewhat sinusoidal. The Haar wavelet which should be very efficient for detecting edge or short term phenomena did not produce equivalent results, suggesting that the errors do represent slow cyclical effects rather than impulses or sudden transitions.

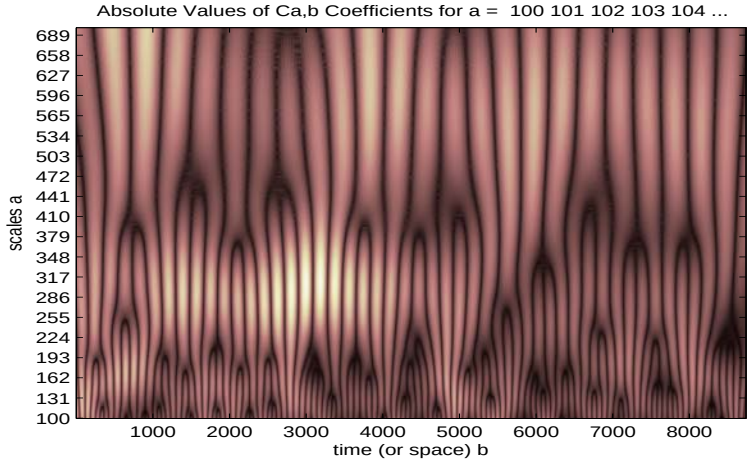

Figure 4.35 Morlet CWT for Atlanta Altitude Error, Week 1264-1265

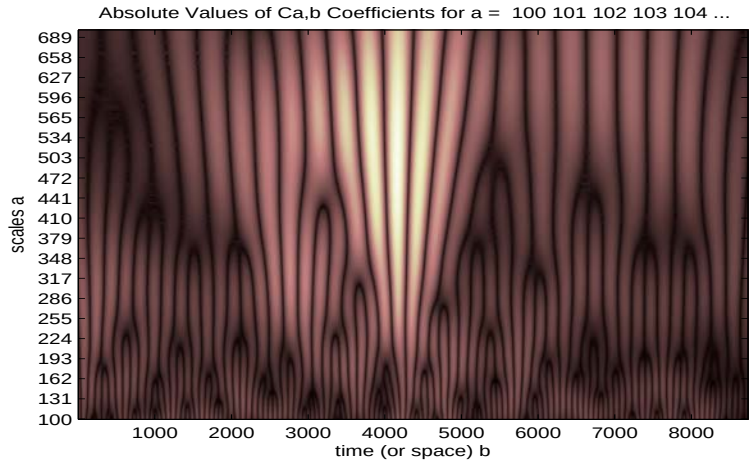

Figure 4.36 Morlet CWT for Atlanta Latitude Error, Week 1264-1265

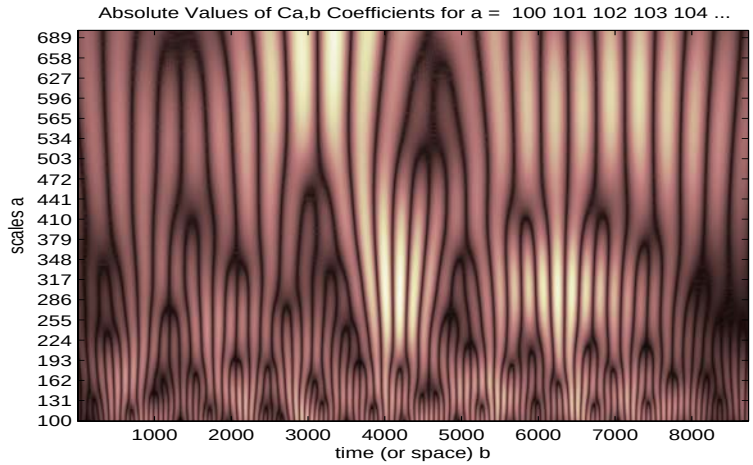

Figure 4.37 Morlet CWT for Atlanta Longitude Error, Week 1264-1265

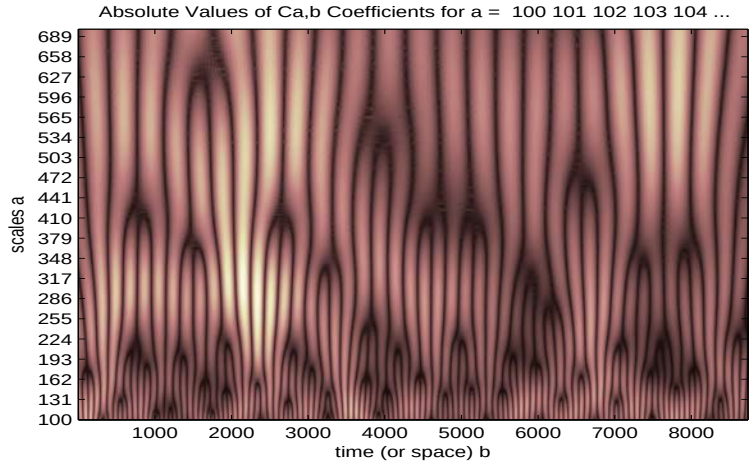

Figure 4.38 Morlet CWT for Oklahoma City Altitude Error, Week 1264-1265

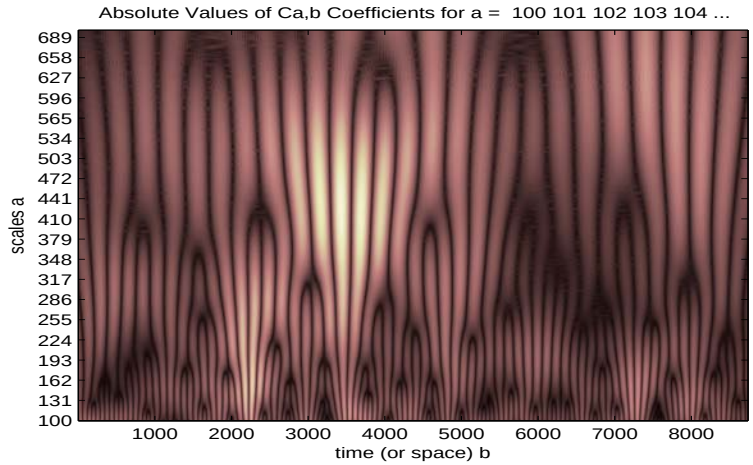

Figure 4.39 Morlet CWT for Oklahoma City Latitude Error, Week 1264-1265

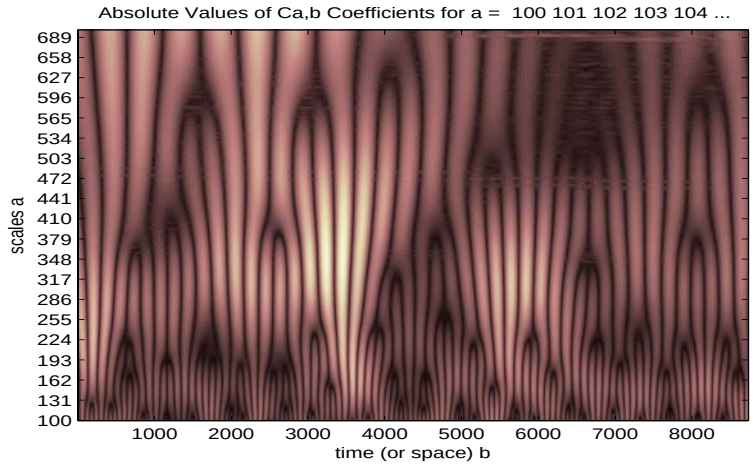

Figure 4.40 Morlet CWT for Oklahoma City Longitude Error, Week 1264-1265

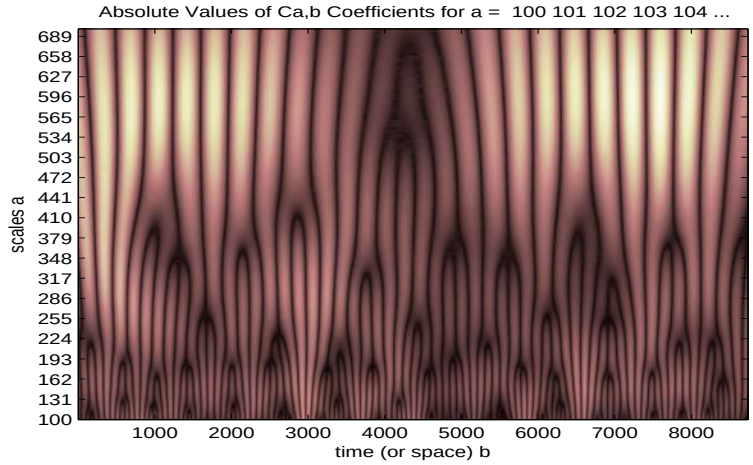

Figure 4.41 Morlet CWT for Los Angeles Altitude Error, Week 1264-1265

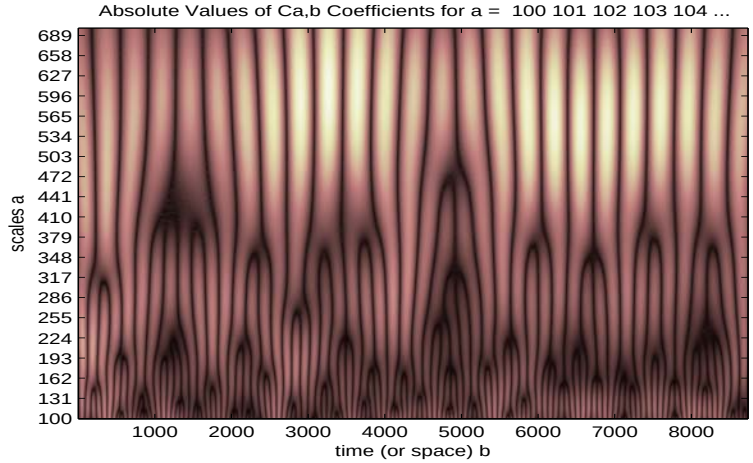

Figure 4.42 Morlet CWT for Los Angeles Latitude Error, Week 1264-1265

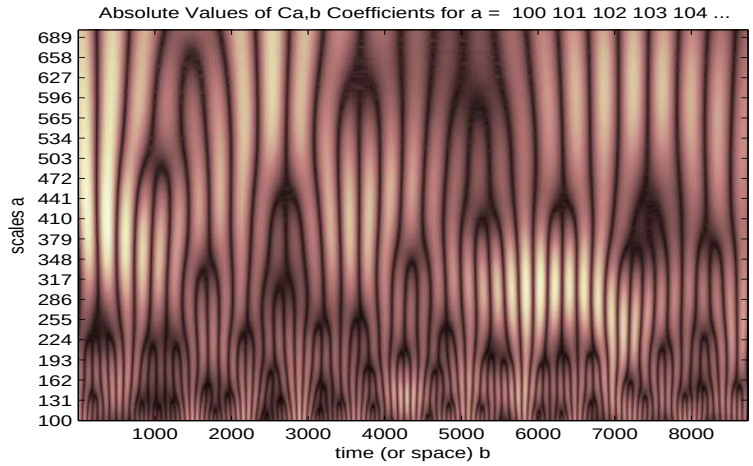

Figure 4.43 Morlet CWT for Los Angeles Longitude Error, Week 1264-1265

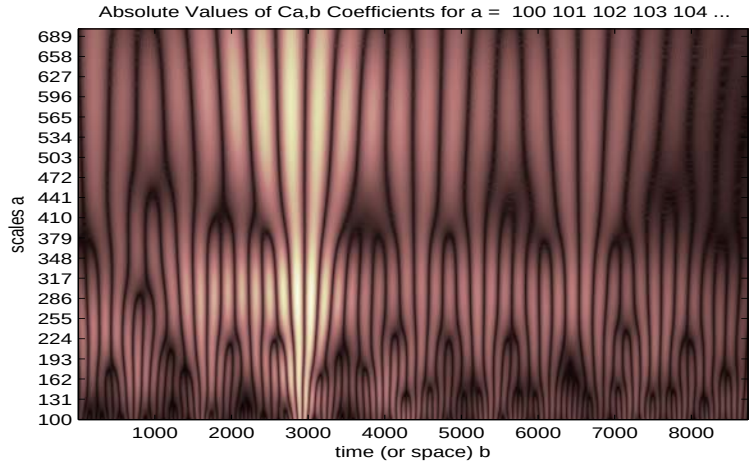

Figure 4.44 Morlet CWT for Minneapolis Altitude Error, Week 1264-1265

4.4 Analysis of Recent WAAS Data

As mentioned earlier, all of the data analyzed to this point was collected five to ten years ago and there have been significant upgrades and enhancements to the WAAS infrastructure since then. An important question to answer before dedicating too many resources to the implementation of additional corrections to the WAAS signal is whether the errors are still present and still significant. To answer this question, a month of WAAS data was collected at the University GPS lab and examined. Because the native format of the collection system was earth-centered, earth-fixed (ECEF), there is not a direct correspondence between this data and the previous sets but because of the position of the lab on the surface of the earth, the discrepancies between the two are not large. The alignment of the ECEF *x* error component is very close the longitudinal error of the earlier data, the ECEF *y* is close to the altitude error, and the ECEF *z* is close to the latitude error.

Both FFT and wavelet analyses were performed on the data. Figure 4.45 is a plot of the lowest 40 frequencies examined by the FFT. In one axis or another, the figure shows the peaks corresponding to the daily and orbital components as well as the 8-hour period signal. The amplitudes of the peaks are actually greater than those seen in the older data.

Figures 4.46 through 4.48 are the CWT plots for the *x*, *y*, and *z* data. As in the FFT plot, there is good agreement with the older data in terms of where the right numbers of bands occur to support the existence of the daily and orbital period sinusoids. The intensities of the correlation values also match up with the peaks in the FFT. The *z* component seems to have no significant daily component but a very

strong orbital one based on the FFT and the CWT plot shows a bright band in the region of scale factor 270, corresponding to the orbital period. The FFT for the *x* component has a much stronger daily component and the highest correlation values in the CWT plot are along the scale factor 540 band.

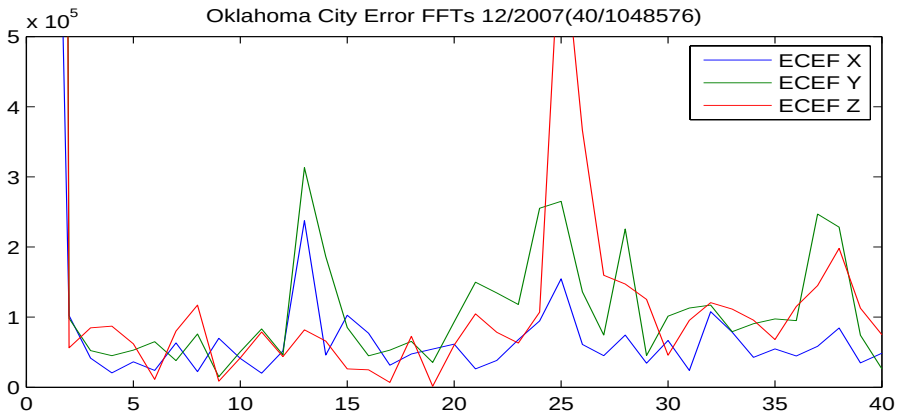

Figure 4.45

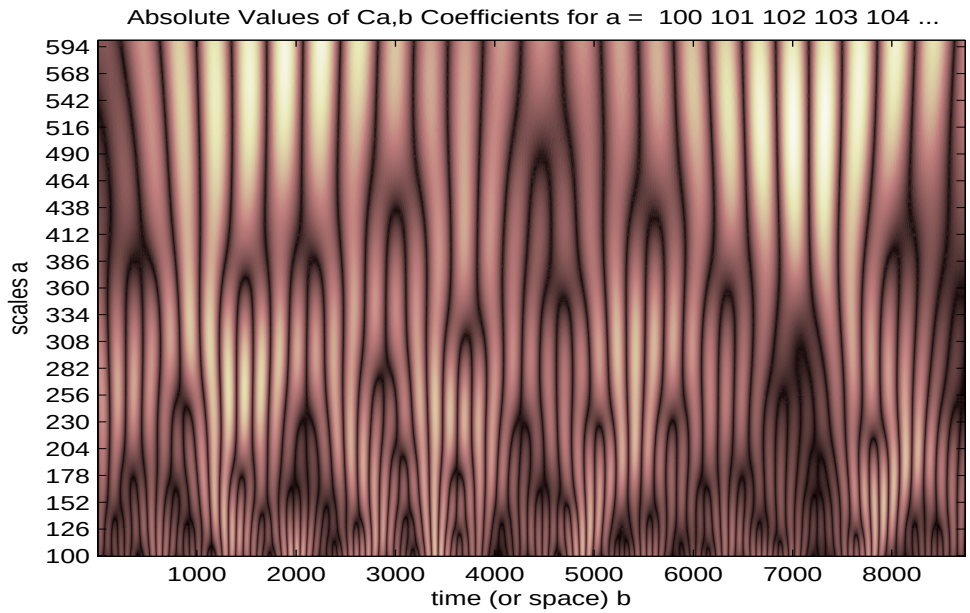

Figure 4.46 Morlet CWT for OKC ECEF *x* Error

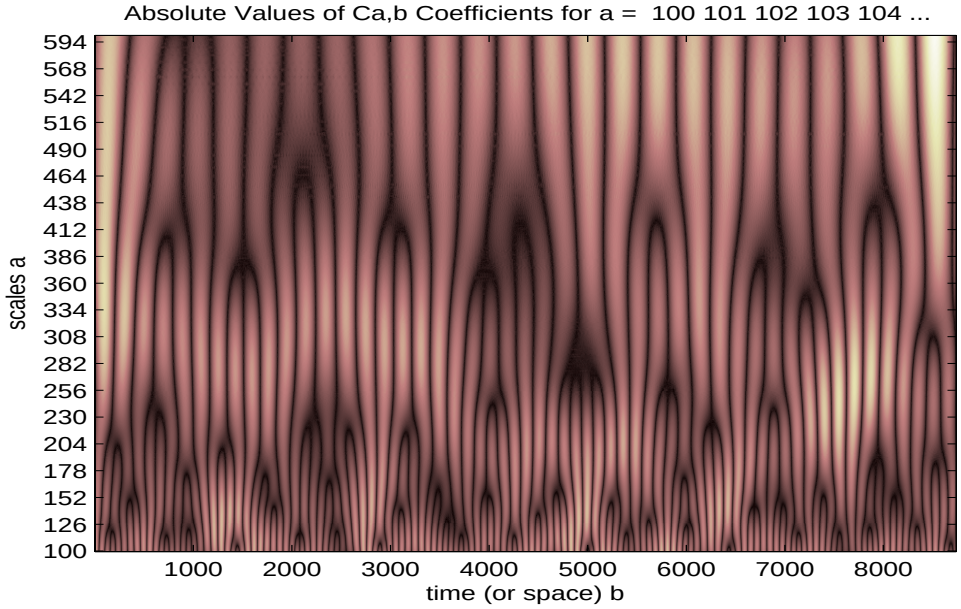

Figure 4.47 Morlet CWT for OKC ECEF *y* Error

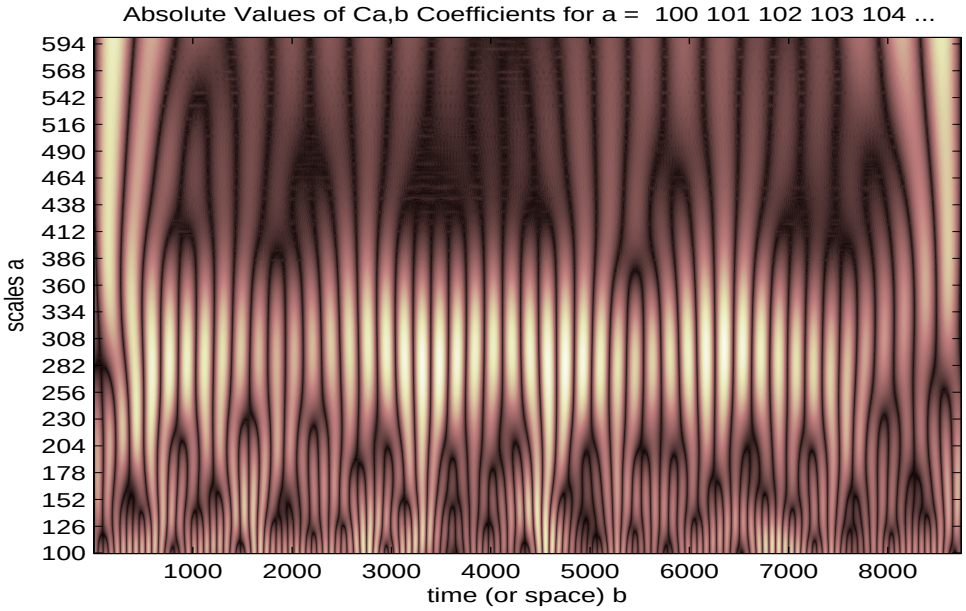

Figure 4.48 Morlet CWT for OKC ECEF *z* Error

This analysis supports the continued existence of the same error components that were present in the original data. While the overall accuracy of the system has been improved by the enhancements to the infrastructure, whatever phenomena are creating the errors identified here remain in effect.

Chapter 5

Results and Conclusions

Considerable evidence has been presented to support the existence of at least two newly observed principal spectral components to the Wide Area Augmentation System position calculation error. The magnitudes of these components represent a significant portion of the total error and their reduction or elimination would represent a substantial improvement in the quality of the system performance. The periods of these two components correspond to the rotation of the earth (around which the GPS satellites that provide data for the WAAS position calculation orbit) and the orbits of those GPS satellites. Possible causes of these errors include systematic errors in the ionospheric or tropospheric models used by the WAAS correction calculation software or multipath phenomena producing errors in the pseudorange data used by that software. Another possible explanation involves orbital deviations in the GPS satellites that are not included in their almanac broadcasts. These deviations, which are of the same order of magnitude as the WAAS errors being studied, are discussed in detail in reference 37, “Determination of the accuracy of the Global Positioning System’s broadcast orbit and the WAAS-corrected orbit.”

As discussed in Chapter 2, any significant reduction in the WAAS error budget could have significant impacts on the systems acceptability as a primary means of navigation for all phases of flight, including precision approach. This is especially true when considered in combination with earlier work done at the University on improving the integrity and availability of the system. That work suggested

enhancements to the current algorithms, which involve a number of worst case estimates and produce “possible” error values that are well outside the observed performance of the system. By simultaneously improving the integrity and accuracy capabilities of the system, a receiver taking advantage of these two enhancements would be a significant step forward for the implementation of WAAS.

The existence of repeatable and predictable errors at WAAS locations across the National Airspace System could be addressed by several methods. Receivers could be provided a database of additional corrections to apply based on location and time of day or orbital position of certain satellites. The ionospheric model in the WAAS system software could be modified to either provide an improved iono thickness or just have predetermined corrective factors added to compensate for errors of unknown origin. If the orbital perturbations mentioned earlier can be shown to be a significant contributor to the error components addressed here, then it might be appropriate to enhance the almanac broadcast to provide better information on the satellite orbits or at least to include information on known predictable perturbations to the WAAS system software. The variations in the error magnitudes that were discussed in section 4.2 as functions of time make the problem more complicated in that they make periodic updates to the correction terms necessary. In the absence of a clearly defined predictive function, that would mandate regular updates to any databases that incorporated the corrections.

The only aviation operations really affected by the level of errors being considered are precision approaches. Aviation operators engaged in instrument operations already receive periodic updates to their databases at 56 day intervals. That

might be sufficient to resolve the update problem for that application. If nothing else could be done, airports could generate additional correction messages for the WAAS receivers to use, creating a "local-area wide-area" augmentation.

In summary, the study demonstrated the presence of newly identified repeatable errors in the WAAS position solution that occurred with orbital (11 hours and 58 minutes) and daily (24 hours) periods. A program was developed to show the repeatability by visually displaying error data from equivalent periods as grayscale points on adjacent rows of pixels. This tool clearly indicated error repeatability for the orbit based component but was less conclusive with regards to the 24 hour cycle.

Next, a Fourier analysis involving application of an FFT to extended sequences of error data showed that peaks were almost always present in the frequency domain representation of the error data corresponding to the orbital and daily based errors. The Fourier analysis also revealed a number of other error components that usually corresponded to harmonic frequencies of the 12 hour period errors but these components were not as consistent across the various locations and periods of observation and were usually of lesser magnitude. It was also harder to develop a physical justification for those errors unless it could be tied to the count of satellites and their separation along the orbital planes. Based on the Fourier scaling factors, it appears that the orbital and daily error components may represent from 10 to 25 per cent of the total error amplitude, depending on the location and, perhaps, time of year. While the Fourier analysis showed that the spectral components were present across the NAS and across the year from which data was available, the associated phase data was generally too irregular to connect the errors at different locations or different

times. It was originally hoped that the phase data might be used to show the travel of the daily error across the WAAS coverage area which could then be linked to the transition of the ionosphere from night thickness to day thickness. Unfortunately, the available data did not support this activity.

Lastly, continuous wavelet transforms were applied to the data. Results from a variety of transforms (Haar, Daubechies, Morlet, and others) were studied for various considerations. The wavelet that appeared to show the strongest correlation was the Morlet, which closely resembles a sinusoid. Examination of a number of CWTs consistently showed that the orbital and daily spectral components were present. In almost all cases, the CWT output also implied that other higher and lower frequency components were also present. The CWT output also indicated that the transitions from one high correlation frequency to another were not consistent. The nodes where multiple branches expanded from a single branch were scattered across a range of scale factors which may correspond to the irregular phase data produced by the FFT.

The variations in the error components' amplitude and phase suggest that the proposed correction information, whether received from a broadcast or fetched from a database, will not be a current calculated value but rather some sort of predicted average based on the historical performance of the data in that area for that time. While more operationally challenging, this functionality would still provide a significant improvement in the system capabilities.

Chapter 6

Lessons Learned and Suggestions for Future Research

6.1 Lessons Learned

This study used very "brute force" applications of both Fourier and wavelet analysis to provide evidence supporting the existence of certain newly identified spectral components. The results of the wavelet studies, in particular, indicate that a great deal more information is available if one understood the tools a little better.

6.2 Suggestions for Future Research

There are a host of future research topics generated by this study. Probably the most obvious and most significant is the identification of what is causing the errors. It was initially suggested to the author that everything he saw was due to multipath phenomena. But for reasons given in the study, that explanation was not considered sufficient. But could multipath account for some of the observed errors? Comparing the rate of change of the error components with the shift of satellite orbit position and the effect of that on multipath would be a useful study. It would be very interesting to continue the work done on the accuracy of the WAAS corrected orbits by Mr. Peters [37] and attempt to correlate those errors to the WAAS position errors.

A second group of potential studies could investigate the other apparent error components. Heterodyning was suggested as an explanation of the 8 hour period error but this assumption needs to be verified. Does heterodyning occur between results of equations? Where in the math is the break between the physics that produce heterodyning and mathematical abstraction? And then there are all the other peaks

that are seen in the FFT outputs and the wavelet correlation coefficient plots. Can the satellite spacing around the orbital planes explain some or all of them? What about cross correlation by satellites in different orbits? Is the frequently occurring peak corresponding to a period of 2 or 3 days real, or just spillover from the DC component?

Given that the spectral components exist, what is the best solution for taking advantage of the knowledge? The paper suggests several possibilities but calculating what the optimal corrections are and how to best include them in the WAAS solution calculation are significant implementation details worthy of further study.

Bibliography and References

[1]. Loh, R., Wullschleger, V., Elrod, B., Lage, M., and Haas, F., "The U.S. Wide Area Augmentation System (WAAS)", NAVIGATION, Vol. 42, No. 3, pp. 435-466, Fall 1995.

[2]. RTCA/DO-229B, "Minimum Operational Performance Standards (MOPS) for Global Positioning system/Wide Area Augmentation System Airborne Equipment". RTCA Inc. Document No. RTCA/DO-229B, Washington, October 1999.

[3]. The White House, Officer of the Press Secretary, "Statement by the President regarding the United States' decision to stop degrading Global Positioning System accuracy", May 1, 2000.

[4]. RTCA Special Committee 159 Working Group 2, "Wide Area Augmentation Signal Specification", September 1995.

[5]. Darne, E., "A Static and Dynamic Analysis of the Operational GPS WAAS", Master's Thesis, University of Oklahoma 2000.

[6]. Dai, D., Walter, T., Enge, P., Powell, J.D., "Satellite-based Augmentation System Signal-In-Space Integrity Performance Analysis, Experience and Perspectives", Proceedings of ION GPS-99, pp. 159-170, The Institute of Navigation, Nashville, TN, September 1999.

[7]. Hansen, A., "WAAS Precision Approach Metrics: Accuracy, Integrity, Continuity and Availability", http://waas.stanford.edu/~wwu/walter/WAAS/metrics.html, January 2004.

[8]. "FAA Commissions WAAS", GPS World, pp. 10-13, August 2003.

[9]. Cabler, H., DeCleene, B., "LPV: New, Improved WAAS Instrument Approach", Proceedings of ION GPS-2002, pp. 1013-1021, The Institute of Navigation, Portland, OR, September 2002.

[10]. Axelrad, P., Brown, R.G., "GPS Navigation Algorithms, Chapter 9, Global Positioning System: Theory and Applications", Washington, DC, AIAA, 1996.

[11]. Brown, R.G., Hwang, P. Y. C. "Introduction to Random Signals and Applied Kalman Filtering with MATLAB Exercises and Solutions", New York, NY, John Wiley & Sons, Inc., 1997.

[12]. Mu, Guangwei, "WAAS Error, Integrity and Availability Modeling for GPS Based Aircraft Landing System", Doctoral Dissertation, University of Oklahoma, 2004

[13]. NTSB/WAAS T&E Team, "Wide-Area Augmentation System Performance Analysis Report #2", http://www.nstb.tc.faa.gov/reports/archives/waaspan2.pdf, Jan. 2002.

[14]. NTSB/WAAS T&E Team, "Wide-Area Augmentation System Performance Analysis Report #27", http://www.nstb.tc.faa.gov/reports/waaspan27.pdf, Jan. 2009.

[15]. Fagan, J.E., Sexton, Ralph, Ladecky, Shahar, "Investigation of a Total System Tolerance Model for Precision Approaches Using GPS/Wide Area Augmentation System", Proceedings of International ION Conference, Sept 1998.

[16]. Fagan, J.E., Hejjo, H. Darne, Emmanuel, "A Static and Dynamic Analysis of the Operational GPS WAAS for Use in Precision and Non-Precision Approaches", Proceedings of ION GPS-99, The Institute of Navigation, Nashville, TN, September 1999.

[17]. Fagan, J.E., "Space Based Satellite Augmentation System (SBAS) Category A and B Flight Test Results", Proceedings of OCP, Vol. II, pp. 102-109, International Civil Aviation Organization/Obstacle Clearance Panel, Oct. 9, 2001.

[18]. Fagan, J.E., "Ground Based Satellite Augmentation System (GBAS) Category A and B Flight Test Results", Proceedings of OCP, Vol. II, pp. 110-116, International Civil Aviation Organization/Obstacle Clearance Panel, Oct. 9, 2001.

[19]. Fagan, J.E., Ross, W., Billman, B., McCartor, G., "A Preliminary Comparison Between WAAS and LAAS Flight Test Results During Cat 1 Instrument Approaches to Landing Using Cat A, B, and C Aircraft", Proceedings of ION GPS-2002, pp. 1966-1974, The Institute of Navigation, Portland, OR, September 2002.

[20]. Fagan, J.E., Ross, W., "A Comparison of Low Cost WAAS Sensors as Airborne Navigation PVT Sources", Proceedings of ION GPS-2000, pp. 1668-1678, The Institute of Navigation, Sept. 2000.

[21]. Fagan, J.E., Ross, W., McCartor, G., "Results of Flight Test Program to Develop New Terminal Instrument Procedures for LAAS/GPS Approaches and Guided Missed Approaches Using Category A, B, and C Aircraft", Proceeding of ION GPS-2003, pp. 1812-1822, The Institute of Navigation, Sept 9-11, 2003.

[22]. Fagan, J.E., Mohr, B., McCartor, G., Sexton, R., "Preliminary Results of Flight Test Program to Develop Curved Path Navigator; Set of New Curved Path Approaches to Landing GPS/LAAS and WAAS", Proceeding of ION GPS-2003, pp. 1823-1828, The Institute of Navigation, Sept 9-11, 2003.

[23]. Fagan, J.E., "Precision Approach to Landing Using LAAS/GPS with Category A and B Aircraft", Proceedings of International Aviation Technical Symposium (IATS) 2003, pp. 97-104.

[24]. Fagan, J.E., Mu, G., Havlicek, J., "WAAS Error, Integrity and Availability Models for GPS based Aircraft Landing System", Proceeding of ION GPS-2004, pp. 48-54, The Institute of Navigation, Jan. 14-17, 2004.

[25]. Fagan, J.E., Wen, H., Huang, P., Dyer, J.W., Archinal, A., "Integrating WAAS into LAAS to Improve the Integrity of LAAS", Proceedings of ION GPS-2005, pp. 2050-2056, Sept 13-16, 2005.

[26]. Fagan, J.E., Wen, H., Huang, P., Dyer, J.W., McCartor, G., "Flight Test Results of a MOPS Compliant LAAS System to Provide Guided Straight and Curved Path Departures and Missed Approaches", Proceedings of ION GPS-2005, pp. 2071-2078, Sept 13-16, 2005.

[27]. Fagan, J.E., Dyer, J.W., DeBrunner, V.E., McCartor, G., "GPS-WAAS Static Error Analysis Using Wavelet Decomposition and Spectral Estimation", Proceedings of ION GPS-2005, pp. 1040-1048, Sept. 13-16, 2005.

[28]. Biezad, D.J., "Integrated Navigation and Guidance Systems", AIAA Education Services, 1999.

[29]. Yasuda, Akio, "Satellite Navigation System, GPS", Presentation at Tokyo University of Marine Science and Technology, Oct. 2005, http://www.soi.wide.ad.jp/class/20050026/slides/01/index_59.htm.

[30]. Braasch, Michael, "Characterization of GPS Multipath Errors in the Final Approach Environment", Proceedings of ION GPS-92, pp. 383-394, Sept. 16-18, 1992.

[31]. "GPS – Explained, Sources of Error in GPS, Multipath Effect", http://www.kowoma.de/en/gps/errors.htm.

[32]. FAA Fact Sheet dated Feb. 14, 2007, http://www.faa.gov/news/fact_sheets/news_story.cfm?newsId=8145.

[33]. Press, W.H., Teukolsky, S.A., Vettenling, W.T., Flannery, B.P., "Numerical Recipes in C, The Art of Scientific Computing, Second Edition", Cambridge University Press, 1992.

[34]. Schilling, R.J., Harris, S.L., "Applied Numerical Methods for Engineers Using Matlab and C", Brooks/Cole Thomson Learning, 2000.

[35]. Percival, D.P., Walden, A.T., "Wavelet Methods for Time Series Analysis", Cambridge University Press, 2000.

[36]. Oppenheim, A.V., Schafer, R.W., "Digital Signal Processing", Prentice-Hall, Inc., 1975.

[37]. Peters, B., "Determination of the Accuracy of the Global Positioning System's Broadcast Orbit and the WAAS-Corrected Orbit", University of New Brunswick, Fredericton, 1999.

[38]. Kumar, P., "Wavelet Analysis for Geophysical Applications", Review of Geophysics, Vol. 35, No. 4, pp. 385-412, November 1997.

[39]. Torrence, C., Compo, G., "A Practical Guide to Wavelet Analysis", Bulletin of the American Meteorological Society, Vol. 79, No. 1, pp. 61-78, January 1998.

[40]. Walker, J., "A Primer on Wavelets and Their Scientific Applications, Second Edition", Chapman & Hall/CRC, 1999.

[41]. Fugal, D.L., "Wavelets: A Conceptual, Practical Approach", Class Notes © Space & Signals Technologies, LLC, Applied Technology Institute, 2008.

[42]. "Global Positioning System – Wikipedia, the Free Encyclopedia", http://en.wikipedia.org/wiki/Global_Positioning_System, 10 May 2009.

[43]. "WAAS – Wikipedia, the Free Encyclopedia", http://en.wikipedia.org/wiki/WAAS, 9 April 2009.

Appendix A

Site Information on WAAS Reference Stations

Location	Rcvr Type	Latitude	Longitude	Altitude
Atlanta	Novatel G2	33.379688	-84.296726	261.133
Boston	Novatel G2	42.735720	-71.480425	39.136
Houston	Novatel G2	29.961896	-95.331426	10.902
Los Angeles	Novatel G2	34.603518	-118.083895	763.529
Minneapolis	Novatel IOC	44.637463	-93.152084	262.689
Oklahoma_City	Ashtech Z12	35.404396	-97.619770	374.350
Salt Lake City	Novatel IOC	40.786044	-111.952177	1287.451
Seattle	Millenium	47.543618	-122.318061	-9.558
Kansas City	Novatel IOC	38.880159	-94.790833	305.919
Washington, DC	Novatel IOC	39.101523	-77.542730	80.079